



## The fumarolic CO<sub>2</sub> output from Pico do Fogo Volcano (Cape Verde)

ALESSANDRO AIUPPA (1), MARCELLO BITETTO (1), ANDREA L. RIZZO (2), FATIMA VIVEIROS (3),  
PATRICK ALLARD (4), MARIA LUCE FREZZOTTI (5), VIRGINIA VALENTI (5) & VITTORIO ZANON (3, 4)

### ABSTRACT

The Pico do Fogo volcano, in the Cape Verde Archipelago off the western coasts of Africa, has been the most active volcano in the Macaronesia region in the Central Atlantic, with at least 27 eruptions during the last 500 years. Between eruptions fumarolic activity has been persisting in its summit crater, but limited information exists for the chemistry and output of these gas emissions. Here, we use the results acquired during a field survey in February 2019 to quantify the quiescent summit fumaroles' volatile output for the first time. By combining measurements of the fumarole compositions (using both a portable Multi-GAS and direct sampling of the hottest fumarole) and of the SO<sub>2</sub> flux (using near-vent UV Camera recording), we quantify a daily output of 1060±340 tons CO<sub>2</sub>, 780±320 tons H<sub>2</sub>O, 6.2±2.4 tons H<sub>2</sub>S, 1.4±0.4 tons SO<sub>2</sub> and 0.05±0.022 tons H<sub>2</sub>. We show that the fumarolic CO<sub>2</sub> output from Pico do Fogo exceeds (i) the time-averaged CO<sub>2</sub> release during 2015-type recurrent eruptions and (ii) is larger than current diffuse soil degassing of CO<sub>2</sub> on Fogo Island. When compared to worldwide volcanoes in quiescent hydrothermal-stage, Pico do Fogo is found to rank among the strongest CO<sub>2</sub> emitters. Its substantial CO<sub>2</sub> discharge implies a continuous deep supply of magmatic gas from the volcano's plumbing system (verified by the low but measurable SO<sub>2</sub> flux), that becomes partially affected by water condensation and sulphur scrubbing in fumarolic conduits prior to gas exit. Variable removal of magmatic H<sub>2</sub>O and S accounts for both spatial chemical heterogeneities in the fumarolic field and its CO<sub>2</sub>-enriched mean composition, that we infer at 64.1±9.2 mol. % H<sub>2</sub>O, 35.6±9.1 mol. % CO<sub>2</sub>, 0.26±0.14 mol. % total Sulfur (S<sub>T</sub>), and 0.04±0.02 mol. % H<sub>2</sub>.

**KEY WORDS:** *Pico do Fogo volcano, Cape Verde, volcanic gases, CO<sub>2</sub> output.*

### INTRODUCTION

Together with tectonic degassing, subaerial volcanism is the primary outgassing mechanism of mantle-derived CO<sub>2</sub> to the atmosphere (WERNER *et alii*, 2019; FISCHER *et alii*, 2019). Over geological time, tectonic and volcanic degassing have been the primary mechanisms for carbon exchange in and out our planet (DASGUPTA AND HIRSCHMANN, 2010; DASGUPTA, 2013; WONG *et alii*, 2019), ultimately playing a control role on pre-industrial atmospheric CO<sub>2</sub> levels and the climate (VAN DER MEER *et alii*, 2014; BRUNE *et alii*, 2017). Although attempts to estimate the global volcanic CO<sub>2</sub>

output started early back in the 1990s (e.g., GERLACH, 1991), substantial budget refinements have only recently arisen from the 8-years (2011-2019) DECADE (Deep Earth Carbon Degassing; <https://deepcarboncycle.org/about-decade>) research program of the Deep Carbon Observatory (<https://deepcarbon.net/project/decade#Overview>) (FISCHER, 2013; FISCHER *et alii*, 2019).

One key result of DECADE-funded research has been the recognition that the global CO<sub>2</sub> output from subaerial volcanism is predominantly sourced from a relatively small number of strongly degassing volcanoes. AIUPPA *et alii*, (2019) showed that the top 91 SO<sub>2</sub> volcanic emitters in 2005-2015 (those systematically detected from space; CARN *et alii*, 2017) produce a cumulative CO<sub>2</sub> release of ~39 Tg/yr, nearly half of which (~19 Tg CO<sub>2</sub>/yr) is produced by only 7 top-degassing volcanoes. It has also been found, however, that a non-trivial CO<sub>2</sub> output is additionally sustained by fumarolic degassing (FISCHER *et alii*, 2019; WERNER *et alii*, 2019) and groundwater transport (TARAN, 2009; TARAN AND KALACHEVA, 2019) at hydrothermal volcanoes in quiescent stage. These low-temperature (hydrothermal) fumarolic emissions typically release CO<sub>2</sub> in the absence of easily detectable (ultraviolet - UV - spectroscopy) spectroscopy) SO<sub>2</sub>, implying that traditional "indirect" CO<sub>2</sub> flux quantification using the volcanic gas CO<sub>2</sub>/SO<sub>2</sub> ratio proxy in tandem with remotely sensed SO<sub>2</sub> fluxes (e.g. WERNER *et alii*, 2019) cannot be employed; more challenging airborne (WERNER *et alii*, 2009) or ground-based (PEDONE *et alii*, 2014; AIUPPA *et alii*, 2015; QUEISSER *et alii*, 2016) "direct" CO<sub>2</sub> flux measurements are required instead. These technical limitations have prevented us from establishing a robust catalogue for fumarolic CO<sub>2</sub> outputs, as <50 of the several hundred degassing volcanoes in "hydrothermal-stage" worldwide have been measured for their CO<sub>2</sub> flux (WERNER *et alii*, 2019). As a consequence, the extrapolated current inventories for the global fumarolic hydrothermal CO<sub>2</sub> flux (from 15 to 35 Tg CO<sub>2</sub>/yr; FISCHER *et alii*, 2019; WERNER *et alii*, 2019) still involve very large uncertainties. In addition, most of the available information is for low-temperature arc volcanic gases, while much less is known for the fumarolic CO<sub>2</sub> output for non-arc settings (divergent, intra-plate or continental rift; e.g., ILYINSKAYA *et alii*, 2015, 2018).

Pico do Fogo, in the Cape Verde Archipelago, is part of the Macaronesia region, an area of the Atlantic Ocean off the western coasts of Africa, also including the archipelagos of the Azores, Madeira and Canary (Fig. 1). This 2829 m a.s.l high strato-volcano (Fig. 2a), located on the island of Fogo, has been the most frequently erupting volcanic centre of the Macaronesia region in the last 500 years (RIBEIRO, 1960). All historical eruptions occurred on its upper flanks or at its summit crater. Between eruptions,

(1) Dipartimento DiSTeM, Università di Palermo, Italy.

(2) Istituto Nazionale di Geofisica e Vulcanologia, Sezione di Palermo, Italy.

(3) Instituto de Investigação em Vulcanologia e Avaliação de Riscos, University of the Azores, Portugal.

(4) Institute de Physique du Globe de Paris, Université de Paris, France.

(5) Dipartimento di Scienze dell'Ambiente e della Terra, Università di Milano Bicocca, Italy.

Corresponding author e-mail: [alessandro.aiuppa@unipa.it](mailto:alessandro.aiuppa@unipa.it)

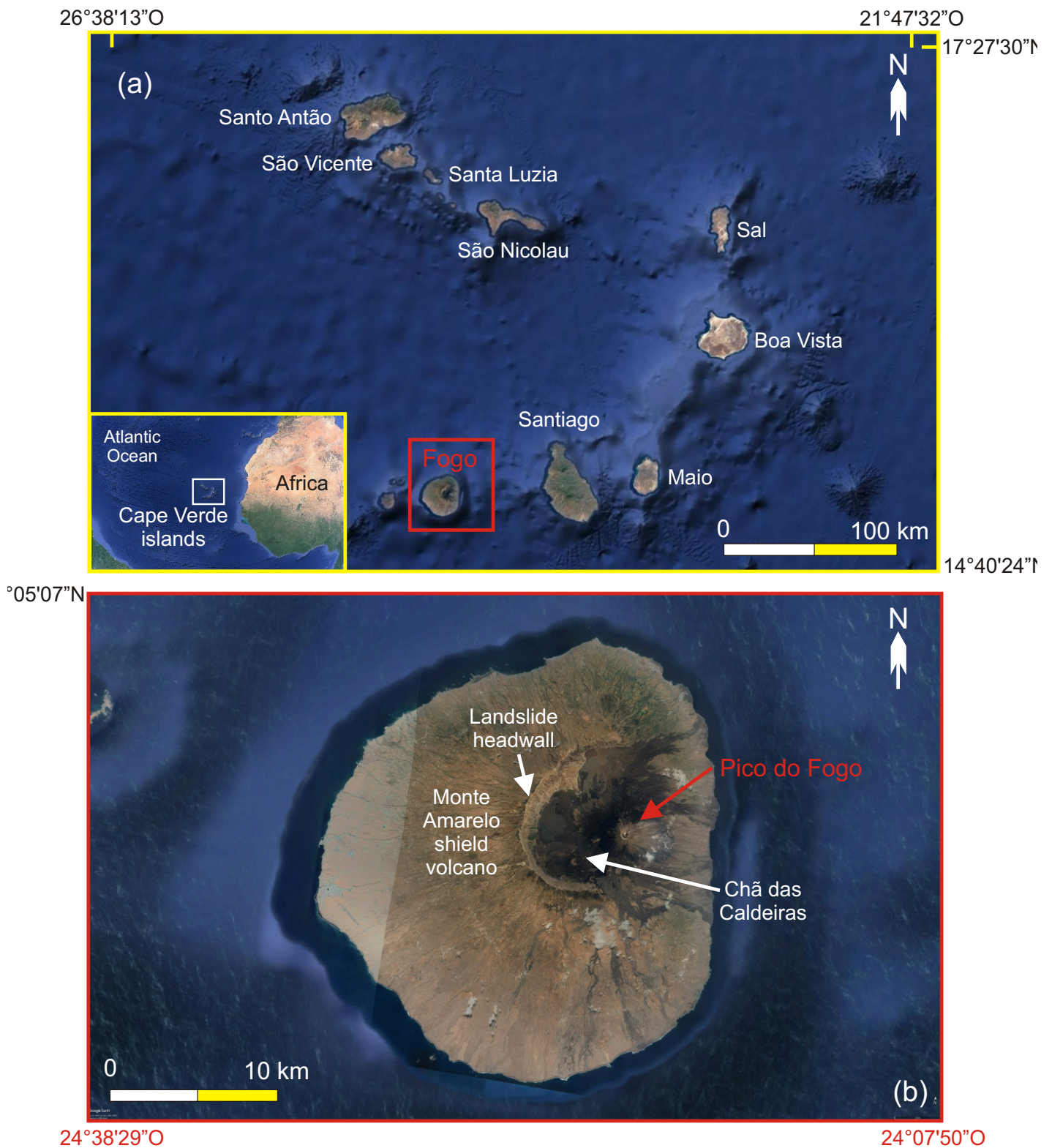
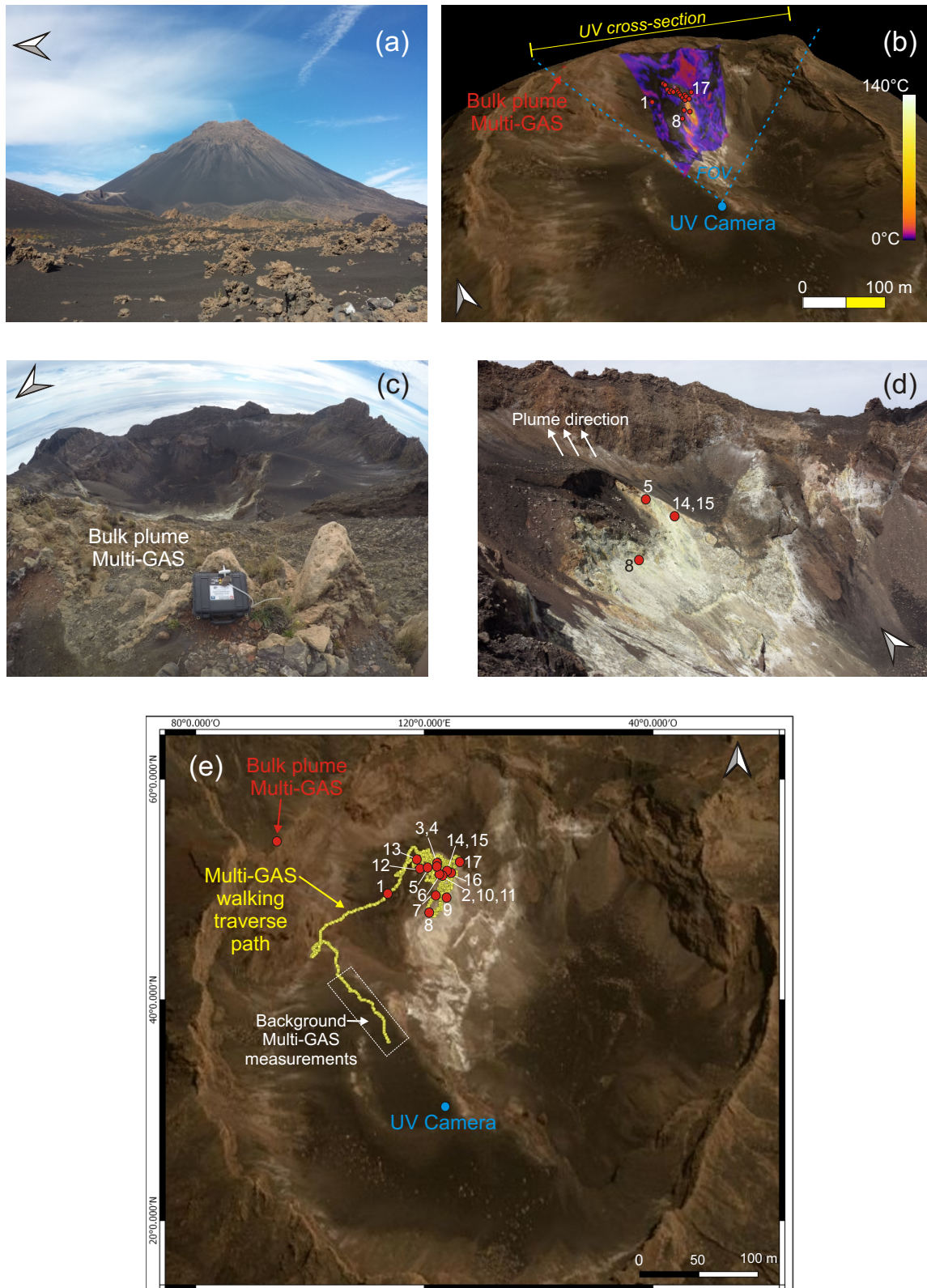


Fig. 1 - Google Earth image (Image © 2019 Maxar Technologies) of (a) the Cape Verde Archipelago and (b) Fogo Island.

the summit crater of Pico do Fogo hosts a persistent fumarolic field (Fig. 2b-e), with several gas vents ranging in temperature from boiling to  $>200^{\circ}\text{C}$  (DIONIS *et alii*, 2014; MELIÁN *et alii*, 2015). The  $\text{CO}_2$  output sustained by diffuse

degassing across the crater floor was estimated in the range  $147\pm 35$  (in 2009) to  $219\pm 36$  t/d (in 2010) (DIONIS *et alii*, 2014, 2015), but no comparable data yet exists for the fumarolic  $\text{CO}_2$  output itself.



*Fig. 2* - (a) Panoramic view of Pico do Fogo Volcano; (b) Map of the Pico do Fogo summit crater, showing (i) a thermal map of the fumarolic field; (ii) the position of the 17 analysed fumaroles (red circles; see (e) for a detail; white numbers identify fumaroles 1, 8 and 17 for reference); (iii) the UV Camera measurement site (FOV and “cross section” are the Field of View of the camera and the ICA integration section, respectively); and (iv) the Bulk-plume Multi-Gas measurement site. The base map is from Bing Maps (<https://www.bing.com/maps>, Microsoft Ltd); (c) the inner crater seen from the Bulk-plume Multi-Gas measurement site; (d) the fumarolic field seen from the UV Camera measurement site. The plume transport direction is indicated by white arrows. The position of some selected fumaroles (red circles with identification numbers) are shown for reference; (e) A zoom of the inner crater (base map as in (a)), showing the track of the Multi-GAS walking traverse and the positions of the 17 fumaroles (red circles with white labels; see Tab 1 for GPS positions). All measurements were performed on February 5, 2019.

Here we fill this gap of knowledge by presenting the very first results for the fumarolic output of CO<sub>2</sub> and other volatiles from Pico do Fogo. These results were obtained from a gas survey on February 5, 2019, during which we combined real-time in-situ measurement of the crater gas compositions (Multi-GAS), direct sampling of the hottest fumarole, and near-vent remote sensing of the SO<sub>2</sub> flux with an UV Camera. Our new data set contributes to improved quantification and understanding of Fogo's quiescent degassing during the multi-decadal phases separating eruptions, and offers an interesting comparison with the gas output measured during the recent 2014–2015 eruption (HERNÁNDEZ *et alii*, 2015). More broadly, our results for Pico do Fogo add a novel piece of information to the still fragmentary data base for fumarolic CO<sub>2</sub> emissions from global volcanoes in hydrothermal stage.

### FOGO ISLAND AND PICO DO FOGO VOLCANO

The Cape Verde Archipelago, extending between 15 and 17°N latitude 500 km to the west of Senegal, is composed of 10 main islands that are the emerged portions of a high oceanic plateau (2 km above the sea floor). Fogo Island is located at the south-western edge of this system (Fig. 1). The Cape Verde oceanic Rise, the world's largest geoid and bathymetric seafloor anomaly (COURTNEY & WHITE, 1986), has been interpreted as due to a hot-spot mantle swell centred north-east of the Sal Island (CROUGH, 1978, 1982; HOLM *et alii*, 2008). The presence of an active mantle plume beneath the northern part of Cape Verde at least has been suggested by some authors based on seismic imaging (MONTELLI *et alii*, 2006; LIU & ZHAO, 2014; SAKI *et alii*, 2015). A mantle plume contribution is also consistent with high primordial <sup>3</sup>He (<sup>3</sup>He/<sup>4</sup>He ratios up to 12.3–15.7 Ra) in volcanics from São Vicente and São Nicolau islands (CHRISTENSEN *et alii*, 2001; DOUCELANCE *et alii*, 2003; MATA *et alii*, 2010; MOURÃO *et alii*, 2012). However, a plume origin for Macaronesian volcanism is still matter of debate (BONATTI, 1990; ASIMOV *et alii*, 2004), and the role of decompressional melting (MÉTRICH *et alii*, 2014) favoured by extensional lithospheric discontinuities (MARQUES *et alii*, 2013) has received increased attention recently. Volcanism at the Cape Verde Islands is thought to have started 24–22 Ma ago on the northeastern islands, followed by a more recent westward migration of volcanic activity (both in the northern and southern branches of the archipelago) during the Pliocene-Pleistocene (HOLM *et alii*, 2008). Erupted products spread a large compositional range but mafic, silica-undersaturated lavas (basanites, tephrites, and nephelinites) prevail (GERLACH *et alii*, 1988; DAVIES *et alii*, 1989; HOLM *et alii*, 2006), eventually associated with rarer carbonatites (KOGARKO *et alii*, 1992; HOERNLE *et alii*, 2002). Trace-element and isotope geochemistry of the erupted volcanics are extremely heterogeneous, with significant differences between the northern and southern islands, implying the probable involvement of several distinct mantle sources: a lower mantle plume containing both mixed HIMU (High  $\mu = {}^{238}\text{U}/{}^{204}\text{Pb}$  at zero age) and EM1 (Enriched Mantle 1) end-members, possibly a 1.6-Ga recycled oceanic crust, plus the depleted upper mantle (northern islands) and the subcontinental lithospheric mantle (southern islands) (GERLACH *et alii*, 1988; DAVIES *et alii*, 1989; HOLM *et alii*, 2006; CHRISTENSEN *et alii*, 2001;

DOUCELANCE *et alii*, 2003; MILLET *et alii*, 2008). The actual relative proportions of each of these sources are still debated however.

Fogo Island (Fig. 1b), formed during the last 3–4.5 Ma, has been the single site of historical volcanic activity (27 reported eruptions) since the discovery of the archipelago in the XV<sup>th</sup> century. The dominant structure of the island is Monte Amarelo Volcano whose summit was truncated by three massive flank collapses between ca. 60 and 43 ka (Fig. 1b) (DAY *et alii*, 1999; 2000; MARQUES *et alii*, 2020). The post-collapse (62 ka to present) activity has been primarily concentrated within the Chã das Caldeiras depression (Fig. 1b), leading to progressive infilling of the collapse scar and the formation of the Pico do Fogo cone. The cone itself (Fig. 2a) has remained the primary eruptive centre until 1785 (RIBEIRO, 1960), when fissure-fed effusive eruptions became concentrated along the flanks of the volcano, occurring at an average frequency of one every ~50 years. The most recent eruptions happened in 1951 (HILDNER *et alii*, 2012), 1995 (HILDNER *et alii*, 2011) and 2014–2015 (CARRACEDO *et alii*, 2015; CAPPELLO *et alii*, 2016; RICHTER *et alii*, 2016; MATA *et alii*, 2017). Eruptive products of the Amarelo-Fogo volcanic complex are primarily alkali-rich tephritic to basanitic lavas (with rarer foidites and more evolved phonolites). They are thought to ascend from a 16–28 km deep magma storage zone, emplaced in the underlying lithospheric mantle (GERLACH *et alii*, 1988; DOUCELANCE *et alii*, 2003; HILDNER *et alii*, 2011, 2012; MATA *et alii*, 2017).

### MATERIALS AND METHODS

On February 5, 2019 we realized extensive field investigations and measurements of the summit crater fumarolic emissions of Pico de Fogo volcano (Fig. 2a–e). We used a portable Multi-component Gas Analyser System (Multi-GAS) to analyse in real-time the fumaroles' compositions during walking traverses across the fumarolic field (see the track shown in Figure 2e). The walking traverse mode, first used on Vulcano Island, in southern Italy (AIUPPA *et alii*, 2005a), is ideal to explore the chemical heterogeneity of a fumarolic field as a high number of fumarolic vents can sequentially be analysed while slowly moving along the path. During the traverse, the Multi-GAS continuously acquired data at 0.5 Hz, and its position was synchronously geo-localized with an embedded GPS. In addition to areas of diffuse soil degassing, 17 main fumarolic vents, showing the strongest emissions, were identified during the traverse (Fig. 2e). Gas composition at each of these vents was determined (Tab. 1) by keeping the MultiGAS inlet at a constant position (and for a few minutes) at about ~50 cm height above the fumarolic vent. Our Multi-GAS instrument comprised the following sensor combination (e.g., AIUPPA *et alii*, 2016): a Gascard EDI030105NG infra-red spectrometer for CO<sub>2</sub> (Edinburgh Instruments; range: 0–30,000 ppmv); 3 electrochemical sensors for SO<sub>2</sub> (T3ST/F-TD2G-1A), H<sub>2</sub>S (T3H-TC4E-1A) and H<sub>2</sub> (T3HYT-TE1G-1A), all from City Technology; and a KVM3/5 Galltec-Mela temperature (T) and relative humidity (Rh) sensor. H<sub>2</sub>O concentration in the fumarolic gases was calculated from co-acquired T, Rh and pressure readings using the Arden Buck equation (see AIUPPA *et alii*, 2016). Reading from the H<sub>2</sub>S sensor were corrected



for 14% cross-sensitivity to  $\text{SO}_2$ . Gas ratios in each of the main fumaroles (Tab. 1) were derived from scatter plots of the gas concentrations using the Ratiocalc software (TAMBURELLO, 2015). Uncertainties in all derived ratios are <15%, except for  $\text{H}_2\text{O}/\text{H}_2\text{S}$  ( $\leq 25\%$ ).

The fumarole 15, displaying the highest emission temperature ( $T = 315^\circ\text{C}$ ), was sampled for dry gases only by inserting a titanium tube 50 cm-long into the vent. This tube was connected to both a quartz line equipped with a condenser in order to remove water vapour and a three-way valve with a syringe allowing to force gas flow into the line. Three dry gas samples were stored in glass bottles equipped of two stopcocks and then moved to the INGV laboratory in Palermo for chemical analysis. Concentrations of He,  $\text{H}_2$ ,  $\text{O}_2$ ,  $\text{N}_2$ , CO,  $\text{CH}_4$ ,  $\text{CO}_2$  and  $\text{H}_2\text{S}$  were determined using a gas chromatograph (Clarus 500, Perkin Elmer) equipped with a 3.5-m column (Carboxen 1000) and a double detector (hot-wire detector and flame ionization detector [FID]).  $\text{SO}_2$  was not measurable with this sampling/analytical setup. Analytical errors were <3%. The results are reported in Tab. 2.

Simultaneously to our Multi-GAS traverse, we also operated a portable dual UV camera system for measuring the volcanic  $\text{SO}_2$  flux. The camera system registered at 0.5 Hz for ~100 minutes from a fixed position on the inner crater terrace's rim, deep inside the summit crater (see Figs. 2b, 2e). The system used two co-aligned cameras (JAI CM-140GE-UV), both fitted with optical lenses of  $45^\circ$  Field of View (FoV), and mounting two different band-pass optical filters with Full Width at Half Maximum (FWHM) of 10 nm and central wavelengths of 310 and 330 nm, respectively. The filters were applied in front of the cameras so to achieve differential UV absorption in the  $\text{SO}_2$  band (KANTZAS *et alii*, 2009; KERN *et alii*, 2010; DELLE DONNE *et alii*, 2019). The system, housed in a peli case and powered by a 12V LiPo battery, was mounted on a tripod and rotated to look upward to image the crater's inner northern slope (where the fumarolic field is located) and a portion of the background sky (Figs. 2b, 2d). Data acquisition was commanded via PC using the Vulcamera software (TAMBURELLO *et alii* 2011). The acquired images (520x676 pixels at 10-bit resolution) were post-processed using standard techniques (KANTZAS *et alii*, 2009; TAMBURELLO *et alii*, 2011, 2012): sets of co-acquired images were combined into absorbance images and were then converted into  $\text{SO}_2$  slant column amount (SCA) images by successively using three different calibration cells. Finally, we derived an Integrated Column Amount (ICA) time-series by integrating the SCA along the cross-section shown in Fig. 2b and then the  $\text{SO}_2$  flux by multiplying the ICA with the plume speed. The plume speed ( $1.9 \pm 0.6$  m/s) was

obtained by processing image sequences acquired at 0.2 Hz using a LifeCam Cinema HD (Microsoft) USB visible camera, integrated in the UV Camera system. Processing involved quantifying the rising speeds of ~50 individual gas puffs of well-resolved structure, moving upward from the fumarolic field toward the crater edge (Fig. 2d).

Finally, from the same position as the UV camera, we used a portable handheld thermal camera (model FLIR E5) in order to acquire a thermal map of the fumarolic field (see Fig. 2b). This map allowed us to verify that the hottest degassing areas were in large part covered by the Multi-GAS traverse. Temperatures of fumaroles 5 and 14-15, the hottest vents in the field (Fig. 2b), were also directly measured in situ with a portable thermocouple.

## RESULTS

### FUMAROLIC GAS COMPOSITION: MULTI-GAS AND DIRECT SAMPLING

As a whole, during the ~74-minute duration of our Multi-GAS traverse, we obtained 4446 simultaneous measurements of  $\text{H}_2\text{O}$ ,  $\text{CO}_2$ ,  $\text{SO}_2$ ,  $\text{H}_2\text{S}$  and  $\text{H}_2$  concentrations in Fogo gas emissions (one analysis every 2 seconds). The entire dataset is illustrated in Figure 3 where the gas concentrations in the near-vent fumarolic plumes are displayed as scatter plots. The concentrations of  $\text{H}_2\text{O}$ ,  $\text{CO}_2$  and  $\text{H}_2$  were corrected for the respective air background values of ~12,000, ~600 and ~0.5 ppmv measured upwind (outside) the fumarolic field (Fig. 2e). The high background  $\text{CO}_2$  concentration compared to "normal" atmosphere (~400 ppmv) is explained by the high diffuse soil  $\text{CO}_2$  emission through the inner crater floor (DIONIS *et alii*, 2014, 2015).

The absolute gas concentrations measured along our traverse display quite large variations (Fig. 3), indicating chemical heterogeneity in the fumarolic field emissions. This is especially evident in the  $\text{SO}_2$  vs.  $\text{H}_2\text{S}$  scatter plot (Fig. 3). Otherwise, one observes broad co-variations among most gas species, even though with some spread. The maximum peak values reached ~23,000 ( $\text{H}_2\text{O}$ ), ~20,000 ( $\text{CO}_2$ ), 118 ( $\text{H}_2\text{S}$ ), 62 ( $\text{SO}_2$ ) and 30 ( $\text{H}_2$ ) ppmv.

The molar compositions of fumarolic gases from the 17 individualized vents (Tab. 1) confirm this spatial heterogeneity. Each fumarole actually exhibited stable, well-resolved composition (see the fumarole 15 example in Figure 3). Instead, the  $\text{SO}_2/\text{H}_2\text{S}$  ratios in all fumaroles span more than three orders of magnitude, from 0.001 to 1.5 (Tab. 1 and Fig. 3). The  $\text{H}_2\text{O}/\text{H}_2\text{S}$ ,  $\text{CO}_2/\text{H}_2\text{S}$ , and  $\text{H}_2/\text{H}_2\text{S}$  also varied considerably within the fumarolic field, with respective ranges of 98-480, 108-240 and 0.05-0.24 (Tab. 1 and Fig. 3).

TABLE 2

Chemistry (in mol %) of major and minor dry gas components in Pico do Fogo F15 fumarole.  $\text{H}_2/\text{H}_2\text{S}$  and  $\text{CO}_2/\text{H}_2\text{S}$  ratios are reported for comparison with the same ratios calculated by Multi-GAS

Sample	T °C	date	He ppm	$\text{H}_2$ ppm	$\text{O}_2$ %	$\text{N}_2$ %	$\text{CH}_4$ ppm	CO ppm	$\text{CO}_2$ %	$\text{H}_2\text{S}$ %	Tot %	$\text{H}_2/\text{H}_2\text{S}$	$\text{CO}_2/\text{H}_2\text{S}$
F15a	315	05/02/2019	8	952	0.11	0.51	0.7	15	97.03	1.03	98.8	0.09	94.20
F15b			8	979	0.33	1.4	1.3	17	95.83	0.96	98.6	0.10	99.82
F15c			6	373	12.63	46.35	2.1	13	39.6	0.37	99.0	0.10	107.03

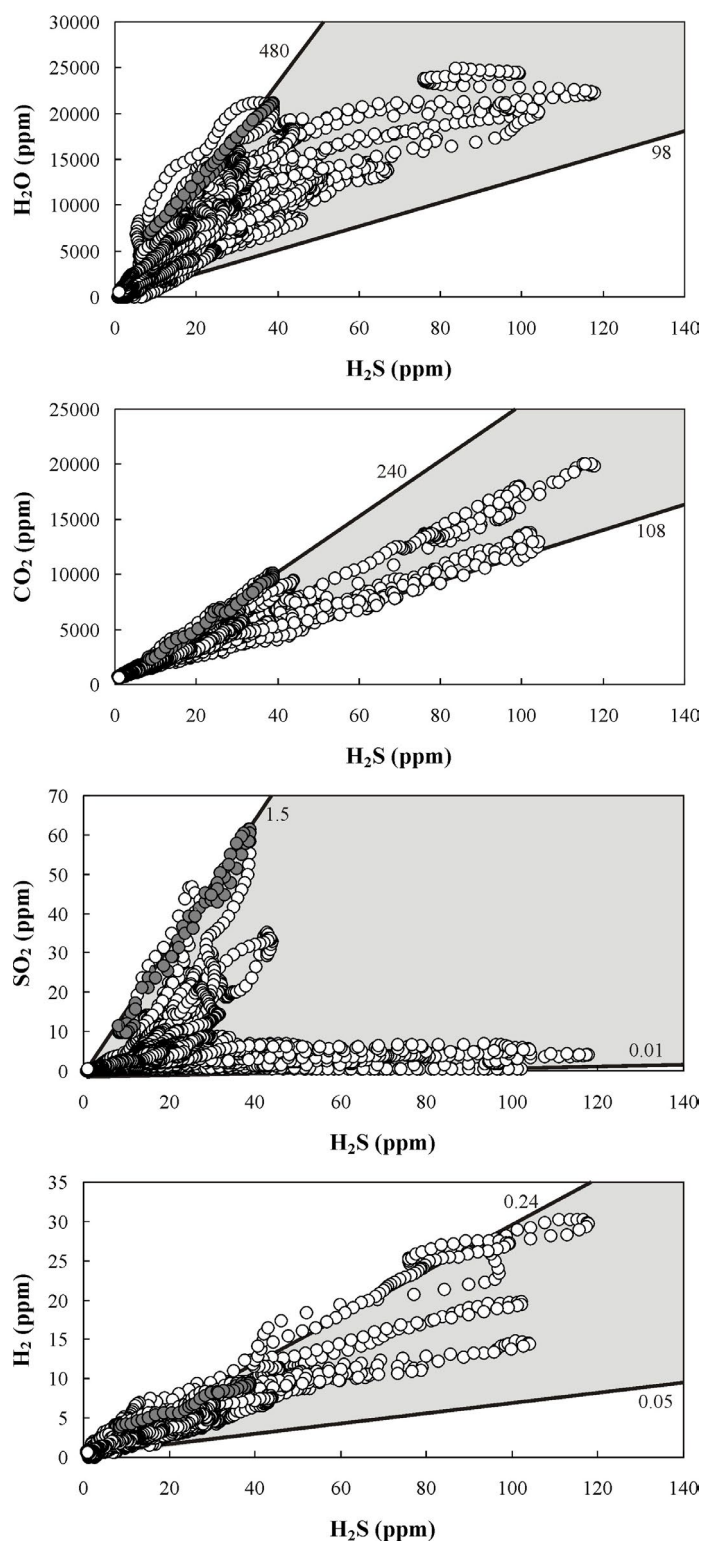


Fig. 3 - Scatter plots of H<sub>2</sub>O, CO<sub>2</sub>, SO<sub>2</sub> and H<sub>2</sub> concentrations vs H<sub>2</sub>S in the plumes of summit crater fumaroles at Pico do Fogo. Open circles stand for the 4446 concentration measurements performed during the ~74-minute-long Multi-GAS walking traverse. H<sub>2</sub>O, CO<sub>2</sub> and H<sub>2</sub> concentrations are corrected for air background (see text). In each plot, solid lines and grey-filled area identify the range (minimum, maximum) of X/H<sub>2</sub>S gas ratios in the identified 17 individual fumaroles (see Table 1). The large spread of compositions, indicated by the large ratio interval (especially for the SO<sub>2</sub>/H<sub>2</sub>S ratio, varying from 0.001 to 1.5), attests to the chemical heterogeneity of the fumarolic field. Otherwise, each of the 17 fumaroles exhibited stable, well-resolved X/H<sub>2</sub>S ratios, as here illustrated by the F15 fumarole example (grey-filled circles).

Table 2 shows the chemistry of dry gases collected from the hottest (315°C) F15 fumarole (Fig. 2d, e). CO<sub>2</sub> is the overwhelming component (up to 97%), followed by H<sub>2</sub>S (around 1%), H<sub>2</sub> (952-979 ppm), CO (15-17 ppm) and CH<sub>4</sub> (around 1-2 ppm). N<sub>2</sub> and O<sub>2</sub> contents reflect air contamination of the samples, with minimum values of 0.5% and 0.1%. The concentration of helium is around 8 ppm in our less contaminated sample. Whatever the degree of air contamination, our samples from the hottest F15 fumarole reveal CO<sub>2</sub>/H<sub>2</sub>S (94-107) and H<sub>2</sub>/H<sub>2</sub>S (0.09-0.10) ratios (Tab. 2) that are very comparable to the corresponding ratios determined with Multi-GAS.

The SO<sub>2</sub>/H<sub>2</sub>S ratio is a commonly used marker to distinguish the magmatic (SO<sub>2</sub>-rich) vs. hydrothermal (H<sub>2</sub>S-rich) nature of volcanic gas (e.g. AIUPPA *et alii*, 2005b). Figure 4 shows that Pico do Fogo fumaroles define a nearly continuous trend from two end-members:

- i. a magmatic end-member, represented by the hottest gas from fumaroles 14-15 (T = 315-316 °C), characterized by H<sub>2</sub>O/CO<sub>2</sub> of ~ 2, CO<sub>2</sub>/S<sub>i</sub> of ~ 100, high SO<sub>2</sub> (~0.2 mol. %) and relatively low H<sub>2</sub>S, and oxidised (redox conditions of about 1 log unit above the Nickel-Nickel Oxide buffer at ~500°C, estimated from the measured SO<sub>2</sub>/H<sub>2</sub>S ~ 0.9-1.4 and H<sub>2</sub>/H<sub>2</sub>O ~ 0.0004; see methodology in AIUPPA *et alii*, 2011); and,
- ii. a hydrothermal end-member, represented by fumaroles 3-8, that is H<sub>2</sub>S-dominated (~0.35-0.43 mol. %; SO<sub>2</sub>/H<sub>2</sub>S of ~ 0.01-0.2), relatively richer in CO<sub>2</sub> (CO<sub>2</sub>/S<sub>i</sub> > 130 and H<sub>2</sub>O/CO<sub>2</sub> < 1) and more reduced (H<sub>2</sub>/H<sub>2</sub>O > 0.0015) (corresponding to redox conditions close to the FeO-FeO1.5 buffer; GIGGENBACH, 1987).

The red star in Figures 4a-d represents the spatially integrated composition of Pico do Fogo's fumarolic emission, calculated as the arithmetic mean of compositions of the 17 main fumaroles. It is characterized by the following ratios, normalized to H<sub>2</sub>S: SO<sub>2</sub>/H<sub>2</sub>S = 0.3±0.4, H<sub>2</sub>O/H<sub>2</sub>S = 299±109, CO<sub>2</sub>/H<sub>2</sub>S = 153±33 and H<sub>2</sub>/H<sub>2</sub>S = 0.2±0.04 (Tab. 1). The mean SO<sub>2</sub>/H<sub>2</sub>S ratio of ~0.3 is not much different from the SO<sub>2</sub>/H<sub>2</sub>S ratio of 0.12 of the bulk volcanic plume (Tab. 1 and Fig. 4) determined after 30-min continuous Multi-GAS measurements made on the outer crater rim (see "bulk plume Multi-GAS site" in Fig. 2b, e). At that Multi-GAS site, we could intercept only a very dilute plume, rising buoyantly from the fumarolic field inside the crater floor (Fig. 2d). Only small concentrations of H<sub>2</sub>S (~ 1 ppmv) and SO<sub>2</sub> (~ 0.15 ppmv) could be detected, no volcanic H<sub>2</sub>O, CO<sub>2</sub>, or H<sub>2</sub> being resolvable from the air background. Given these very low H<sub>2</sub>S and SO<sub>2</sub> concentrations, well below our calibration range (10-200 ppmv), the inferred bulk plume SO<sub>2</sub>/H<sub>2</sub>S ratio of 0.12 must be considered with caution; we just take it as indication that hydrothermal H<sub>2</sub>S-rich fumaroles prevail over the more magmatic end-member fumaroles in the bulk gas emission from Pico do Fogo, in agreement with indications from the arithmetic mean of fumarolic compositions.

#### SO<sub>2</sub> FLUX

Figure 5a presents the SO<sub>2</sub> flux time-series obtained by the UV Camera on February 5, 2019. A plot of SO<sub>2</sub> column amounts along the UV cross-section of Fig. 5b shows that, thanks to the short distance (~200 m) between the

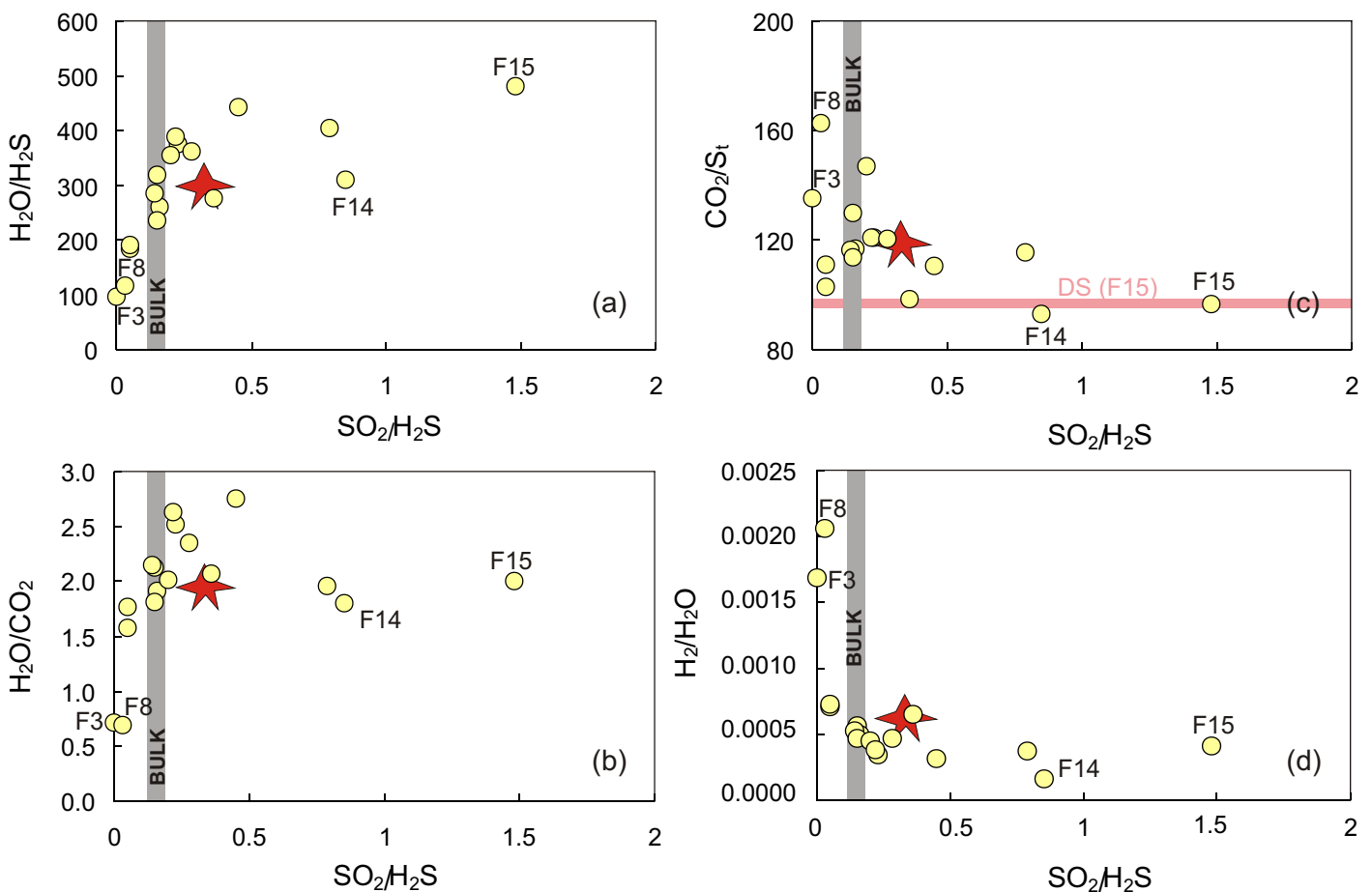


Fig. 4 - Scatter plots of  $\text{SO}_2/\text{H}_2\text{S}$  ratios in the 17 fumaroles vs. (a)  $\text{H}_2\text{O}/\text{H}_2\text{S}$  ratios, (b)  $\text{H}_2\text{O}/\text{CO}_2$  ratios, (c)  $\text{CO}_2/\text{S}_t$  ratios, and (d)  $\text{H}_2/\text{H}_2\text{O}$  ratios (data from Table 1). The  $\text{SO}_2/\text{H}_2\text{S}$  ratio is taken as a good indicator of the magmatic (high- $\text{SO}_2$ ) vs. hydrothermal (high- $\text{H}_2\text{S}$ ) signature of each fumarole. The measured fumaroles define a nearly continuous trend between a “magmatic” gas end-member, represented by the  $\text{SO}_2$ -richer, hydrous ( $\text{H}_2\text{O}/\text{CO}_2 \sim 2$ ) and more oxidised (low  $\text{H}_2/\text{H}_2\text{O}$ ) F14-F15 fumaroles, and a hydrothermal ( $\text{H}_2\text{S}$ -dominated) end-member (exemplified by fumaroles F3-F8), richer in  $\text{CO}_2$  ( $\text{CO}_2/\text{S}_t > 130$  and  $\text{H}_2\text{O}/\text{CO}_2 < 1$ ) and more reduced ( $\text{H}_2/\text{H}_2\text{O} > 0.0015$ ). Note that we directly collected 3 dry-gas samples of fumarole F15 for comparison, which yield a  $\text{CO}_2/\text{S}_t$  ratio range of 94-107 (Table 2; pink horizontal bar labelled “DS” in (c)) nearly identical to the Multi-GAS-derived ratio (97; Table 1). In each plot the red star identifies the average (arithmetic mean of the 17 fumaroles) composition of the fumarolic field (Table 1), while the vertical grey bar (“BULK”) indicates the  $\text{SO}_2/\text{H}_2\text{S}$  ratio measured in the bulk plume from the outer rim (site in Fig. 2).

camera and the targeted plume, a feeble but continuous  $\text{SO}_2$  emission ( $<400$  ppm-m; mean,  $140 \pm 110$  ppm-m) was detected by the UV Camera in the leftmost portion of the camera FoV (Fig. 5c), and persisted throughout the  $\sim 100$  minutes of recording (Fig. 5a). During our measurement interval the  $\text{SO}_2$  flux varied between 0.3 and 2.3 tons/day (or 0.009 to 0.06 kg/s) and averaged at  $1.4 \pm 0.4$  tons/day ( $0.016 \pm 0.004$  kg/s).

## DISCUSSION

### THE COMPOSITION OF PICO DO FOGO FUMARoles

The molar gas ratios determined by Multi-GAS measurements allow to compute the molar percentages of  $\text{H}_2\text{O}$ ,  $\text{CO}_2$ ,  $\text{H}_2\text{S}$ ,  $\text{SO}_2$  and  $\text{H}_2$  in each fumarole and in the mean gas composition (Table 1). These percentages for only the 5 above species are upper bounds since we did not determine other possible minor species ( $\text{N}_2$ ,  $\text{HCl}$ ) in the gases. Otherwise, they are not affected by the presence

of reduced carbon species, whose amount was verified to be very low in F5 fumarole this study and (MELIÁN *et alii*, 2015). According to our results, the Pico do Fogo fumaroles are moderately hydrous (41-73 %  $\text{H}_2\text{O}$ ; mean, 64 %),  $\text{CO}_2$ -rich (27-59 %; mean, 36 %), and contain about  $\sim 0.3$  %  $\text{S}_t$  and 0.04 %  $\text{H}_2$  (Tab. 1). These mean values match well the composition of the F15 fumarole, directly sampled and analysed in laboratory, as regards the  $\text{H}_2/\text{H}_2\text{S}$  and  $\text{CO}_2/\text{H}_2\text{S}$  molar ratios (Tab. 2).

The triangular plot in Figure 6 puts the  $\text{H}_2\text{O}-\text{CO}_2-\text{S}_t$  compositions of our Pico do Fogo fumaroles in a wider context, by comparing them against the compositions of (i) the 2014 Fogo eruption plume (HERNÁNDEZ *et alii*, 2015), which represents the only available datum for the Fogo magmatic gas signature to date; (ii) magmatic gases from other intraplate, rift and/or divergent-plate volcanoes (see AIUPPA, 2015 for data sources); and (iii) fumaroles from other volcanic systems in the Macaronesia region, including the Azores (CALIRO *et alii*, 2005; FERREIRA & OSKARSSON, 1999; FERREIRA *et alii*, 2005; MARES project, this study) and Teide in the Canary (MELIÁN *et alii*, 2012;

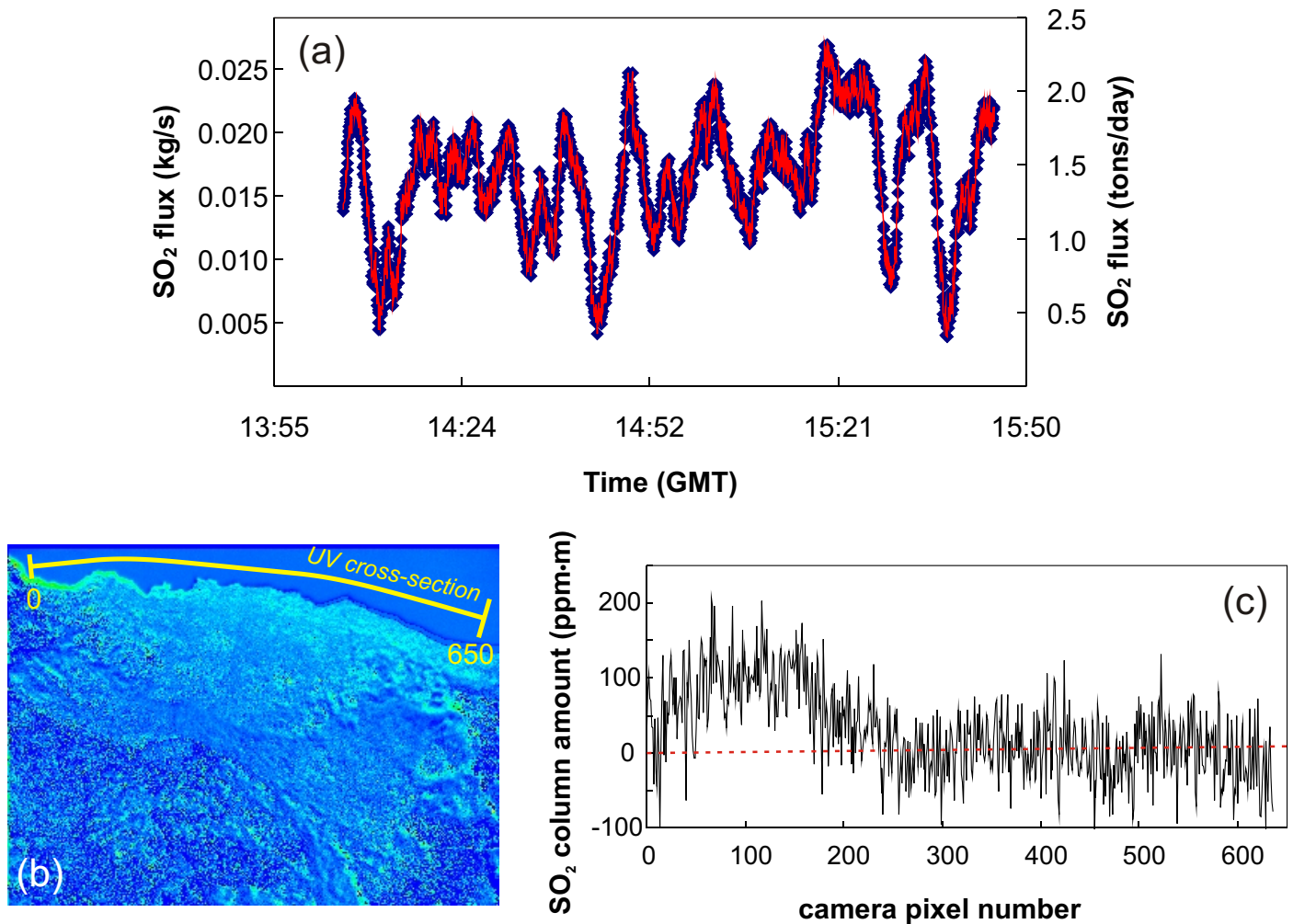


Fig. 5 - (a) SO<sub>2</sub> flux time-series obtained with the UV Camera from the “UV Camera” measuring site indicated in Figure 2. Blue diamonds are individual data (obtained every 2 seconds) while the red line is for a 60 sec mobile average; (b) a pseudo-colour image obtained by combination of two simultaneously taken (by the two co-exposed UV cameras) images, showing the inner crater wall, and the ICA integration section (UV cross-section); (c) an example of SO<sub>2</sub> column amount (in ppm-m) variation along the camera pixels over the UV cross-section shown in (b). The plume is identified by higher-than-background SO<sub>2</sub> column amounts (0-400 ppm-m) between camera pixels 0 and ~200.

MARES project, this study).

The Pico do Fogo summit fumaroles are compositionally distinct from the magmatic gases released during the 2014 eruption (HERNÁNDEZ *et alii*, 2015), this latter falling well within the range of measured magmatic gas compositions at other intraplate volcanoes (yellow field, from AIUPPA, 2015). More specifically, the summit Fogo fumaroles are evidently S-depleted relative to the 2014 magmatic gas, which strongly suggests intense sub-surface scrubbing of reactive S compounds under the “hydrothermal” conditions of the fumarolic field, where surface temperatures ( $\leq 315$  °C) are well below the boiling temperature of liquid sulfur (455 °C; above which S scrubbing become minimal, if any; AIUPPA *et alii*, 2017). Extensive S deposition in the sub-surface environment of the summit fumaroles is further supported by CO<sub>2</sub>/S<sub>i</sub> ratios being far higher in the fumaroles (93-162) than in the 2014 eruption gas (1.5; HERNÁNDEZ *et alii*, 2015) (Figs. 6, 7). The two hottest summit fumaroles (F14 and F15) consistently display the lowest CO<sub>2</sub>/S<sub>i</sub> ratios (93-97), but these are still two orders of magnitude higher than in the eruptive gas, confirming the importance of sulfur scrubbing (Fig. 7). This is also verified for the dry gases

directly sampled from fumarole F15, whose CO<sub>2</sub>/H<sub>2</sub>S ratio is 94-107 (Tab. 2).

Fogo summit fumaroles are also less hydrous (or more CO<sub>2</sub>-rich) than the 2014 eruptive gas (Fig. 6). If the 2014 gas is representative of the magmatic gas feeding the summit fumaroles (a magmatic gas supply is indeed supported by the low but measurable SO<sub>2</sub> output; Fig. 5), then the simplest explanation of H<sub>2</sub>O depletion in the fumaroles is extensive steam condensation in the fumarolic conduits due to low temperature conditions. Because our Multi-GAS measurements were made in air-diluted (and cooled) fumarolic plumes, we cannot entirely exclude that partial H<sub>2</sub>O condensation could have also occurred during plume transport and/or in the Multi-GAS inlet system (tubing + filter), such as previously observed at other volcano-hydrothermal systems (e.g., ALLARD *et alii*, 2014; LOPEZ *et alii*, 2017; TAMBURELLO *et alii*, 2019). However, we note that our Multi-GAS-derived H<sub>2</sub>O range (41-73 %) partially overlaps with the H<sub>2</sub>O range (52-92 %) for the summit Fogo fumaroles previously determined from direct gas sampling (MELIÁN *et alii*, 2015). We thus conclude that both subsurface and within-plume H<sub>2</sub>O condensation may

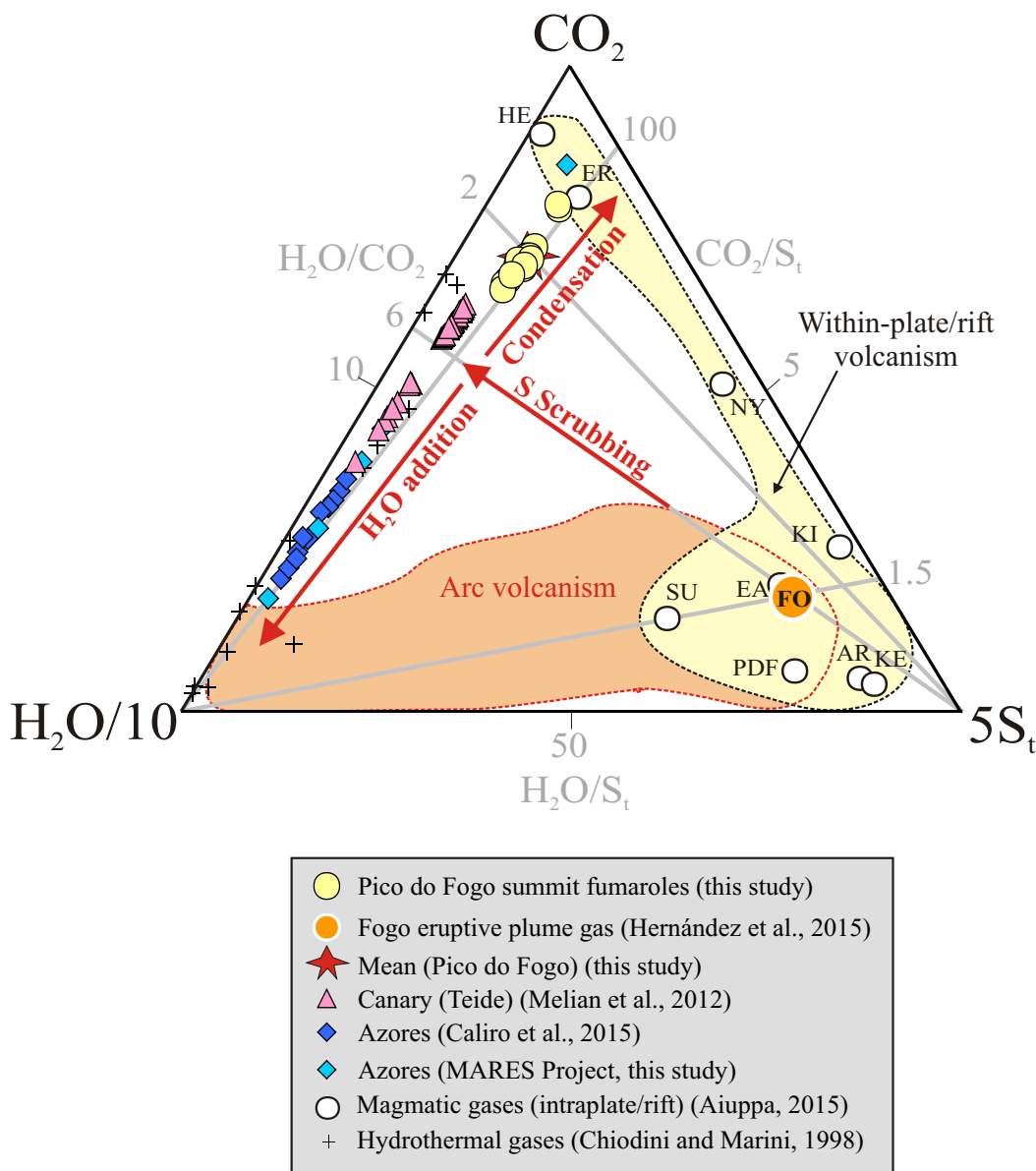


Fig. 6 -  $\text{H}_2\text{O}/10\text{-CO}_2\text{-}5\text{S}_t$  triangular plot comparing the compositions of Pico do Fogo summit fumaroles (yellow circles, data from Table 1; red star mean composition as in Figure 4) with the compositions of (i) the 2014-2015 Fogo eruptive plume (orange circle labelled "FO"; HERNÁNDEZ *et alii*, 2015) (ii) hydrothermal vents from the Macaronesia (see legend) and worldwide (crosses; CHIODINI & MARINI, 1998). Also shown for comparison are the compositional fields of arc magmatic gases and intraplate/rift magmatic gases (AIUPPA, 2015). The white circles identify compositions for some intraplate/rift volcanoes (HE: Hekla; ER: Erebus; NY: Nyiragongo; KI: Kilauea summit; KE: Kilauea east rift zone; AR: Ardoukoba; PDF: Piton de la Fournaise; EA: Erta Ale; SU: Surtsey; see AIUPPA, 2015 for data provenance). Grey lines identify some characteristic  $\text{CO}_2/\text{S}_t$  and  $\text{H}_2\text{O}/\text{CO}_2$  ratios (see grey numbers on axes). The effects of S scrubbing,  $\text{H}_2\text{O}$  condensation or addition are illustrated by the red lines (with arrows).

combine to drive the summit fumaroles toward a less hydrous and correspondingly  $\text{CO}_2$ -enriched composition compared to the 2014 eruptive gas. We cannot exclude, however, that the magmatic gas that feeds the persistent summit fumaroles is compositionally different from the 2014 eruptive gas. If for example the magmatic gas source is the Pico do Fogo magma reservoir located in the uppermost mantle at 16–28 km depth (HILDNER *et alii*, 2011, 2012; MATA *et alii*, 2017), then it is well possible that its composition has deeper ( $\text{CO}_2$ -richer,  $\text{H}_2\text{O}$ -S-poorer) signature than that of eruptive 2014 gas (derived from shallow degassing).

The Pico do Fogo fumaroles plot at the  $\text{CO}_2$ -rich end of the compositional array defined by volcanic hydrothermal fluids in the Macaronesia region (Fig. 6). The majority of volcanic fumaroles from the Azores (São Miguel, Terceira and Graciosa islands) and from Teide volcano in the Canari are shifted toward the  $\text{H}_2\text{O}$  corner. This is a typical (but not exclusive) feature of most hydrothermal steam vents

worldwide (CHIODINI & MARINI, 1998), which reflects their derivation from the boiling of meteoric groundwater-fed hydrothermal systems (CALIRO *et alii*, 2015). The less hydrous compositions of Pico do Fogo fumaroles suggest the absence of a shallow boiling hydrothermal aquifer underneath Fogo summit, and consequently a weaker (relative to Azores and Teide) hydrothermal fingerprint (greater magmatic signature), especially in the hottest fumaroles (F14 and F15) that also exhibit lower  $\text{CO}_2/\text{S}_t$  ratios (Fig. 7) and higher  $\text{SO}_2/\text{H}_2\text{S}$  ratios (Fig. 4). These  $\text{SO}_2$ -bearing F14-F15 fluids appear as formerly magmatic gases that have undergone partial  $\text{H}_2\text{O-S}_t$  loss (via condensation + scrubbing) during cooling and hydrothermal re-equilibration (Fig. 6). Instead, the most  $\text{SO}_2$ -poor,  $\text{H}_2\text{S}$ -dominated fumaroles (e.g., F3-F8) have suffered more significant hydrothermal processing, as testified by their lower  $\text{H}_2\text{O}/\text{CO}_2$  (< 1), higher  $\text{CO}_2/\text{S}_t$  (> 130), and more reduced ( $\text{H}_2$ -rich) redox conditions, typical of hydrothermal fluids (FISCHER & CHIODINI, 2015) (Figs. 4, 7).

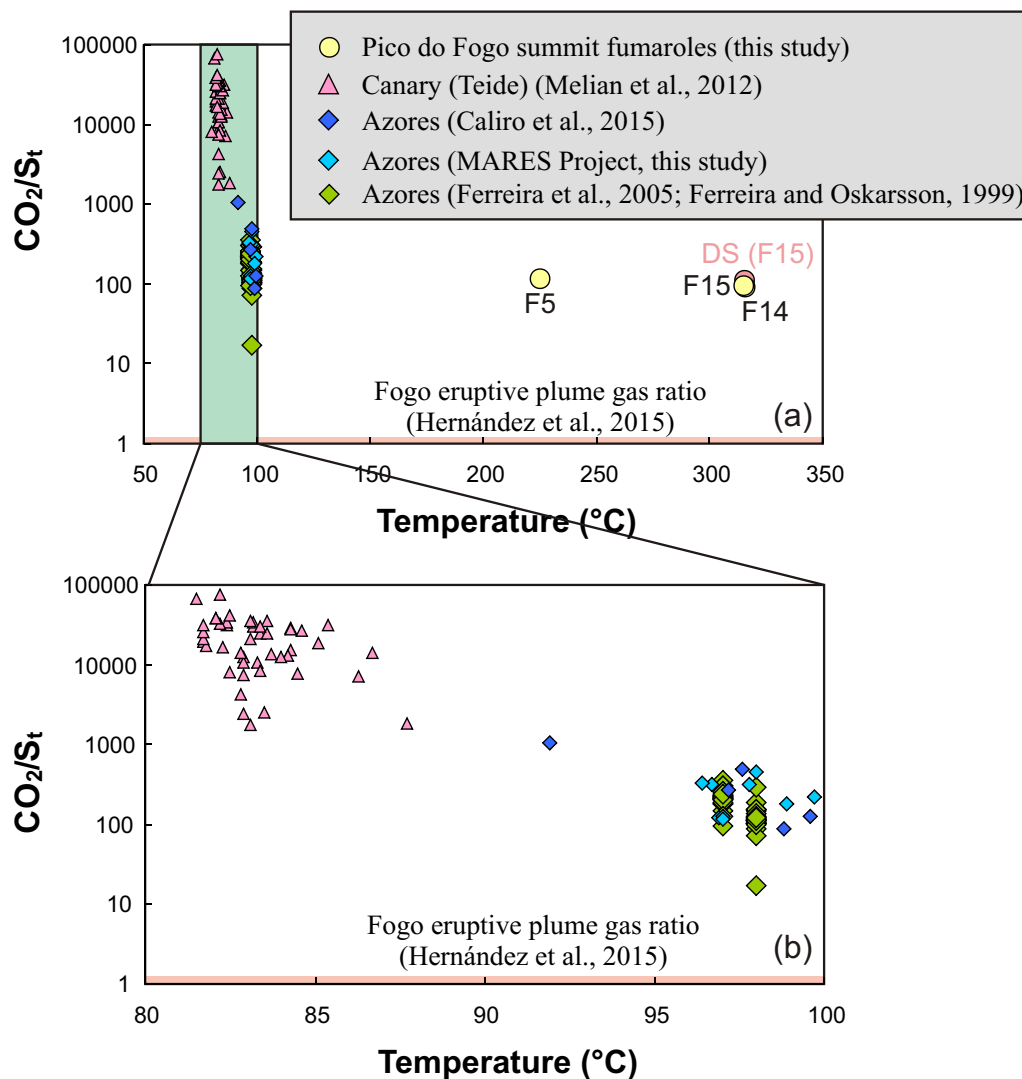


Fig. 7 - (a) Temperature dependence of  $\text{CO}_2/\text{S}_t$  (molar) ratios in the Macaronesia fumarolic gas samples. At Pico do Fogo, we measured temperatures (with a thermocouple) in only the three hottest vents (F5, F14 and F15). The  $\text{CO}_2/\text{S}_t$  (molar) ratios in hydrothermal fluids from volcanoes in the Azores and from Teide (Tenerife, Canary) are shown for comparison in both (a) and in the zoom of (b). The latter shows that  $\text{CO}_2/\text{S}_t$  ratios in fumaroles from Azores-Canary are negatively correlated with temperature, as observed globally (AIUPPA *et alii*, 2017). For reference, we also show in both panels the  $\text{CO}_2/\text{S}_t$  ratio signature of Fogo magmatic gas, as determined by Multi-GAS plume measurements during the 2014-2015 eruption (HERNÁNDEZ *et alii*, 2015; see also Figure 6).

To conclude, we attribute the  $\text{CO}_2$ -rich compositions of the Pico do Fogo fumaroles to a combination of (i) hydrothermal interactions (partially removing magmatic sulphur and water) and possibly (ii) a deep magmatic gas source.

#### GAS OUTPUT BUDGET

Combining the compositional data described above with the UV camera-based  $\text{SO}_2$  flux record depicted in Figure 5, we can reliably estimate the output of  $\text{CO}_2$  and other volatiles from the summit crater fumarolic field of Pico do Fogo (Table 3). To do this calculation, we combine the measured mean  $\text{SO}_2$  flux ( $1.4 \pm 0.4$  tons/day) and the mean molar composition of the summit fumaroles ( $64.1 \pm 9.2$  %  $\text{H}_2\text{O}$ ,  $35.6 \pm 9.1$  %  $\text{CO}_2$ ,  $0.2 \pm 0.08$  %  $\text{H}_2\text{S}$ ,  $0.06 \pm 0.06$  %  $\text{SO}_2$ , and  $0.04 \pm 0.02$  %  $\text{H}_2$ ; red star in Figs. 4, 6 and 7), the  $\text{S}_t$  ( $0.26 \pm 0.14$  %) of which is scaled to the bulk plume  $\text{SO}_2/\text{H}_2\text{S}$  ratio of 0.12 (Tab. 1 and Fig. 4) to infer the bulk plume mass ratios at 558 ( $\text{H}_2\text{O}/\text{SO}_2$ ), 756 ( $\text{CO}_2/\text{SO}_2$ ), 4.2 ( $\text{H}_2\text{S}/\text{SO}_2$ ) and 1.1 ( $\text{H}_2/\text{SO}_2$ ), respectively. This procedure allows us to smooth the effect of the

large compositional heterogeneity of the fumarolic vents. We just note that the bulk plume  $\text{SO}_2/\text{H}_2\text{S}$  ratio of 0.12 characterizes the predominance of  $\text{H}_2\text{S}$ -dominated (F3-F8-like) hydrothermal fluids over more  $\text{SO}_2$ -rich (F14-F15-like) “more magmatic” fumaroles.

We obtain a daily fumarolic  $\text{CO}_2$  output of  $1060 \pm 340$  tons (Table 3). We also estimate a daily release of  $780 \pm 320$   $\text{H}_2\text{O}$ ,  $6.2 \pm 2.4$   $\text{H}_2\text{S}$  and  $0.05 \pm 0.022$   $\text{H}_2$ . These results demonstrate that the fumarolic gas output is larger, for all volatiles, than diffuse degassing through the crater floor (DIONIS *et alii*, 2014, 2015) (Fig. 8). For example, the latter has been estimated to produce 147-219 ( $\pm 35$ ) tons/day of  $\text{CO}_2$  (DIONIS *et alii*, 2014, 2015), which is only 14-20% of the inferred fumarolic  $\text{CO}_2$  output. Even considering the soil  $\text{CO}_2$  output estimated at the scale of the entire island ( $828 \pm 5$  tons/day; DIONIS *et alii*, 2015), the contribution of diffuse degassing remains less than a half ( $\sim 43\%$ ) of the total Fogo island  $\text{CO}_2$  degassing budget ( $\sim 1890$  tons/day; this study and DIONIS *et alii*, 2015).

In contrast, the daily fumarolic gas output is far lower than the eruptive gas output (Fig. 8) for the 2014 eruption derived by HERNÁNDEZ *et alii*, (2015) by combining  $\text{SO}_2$  flux measurements with a scanning UV spectrometer (using

TABLE 3

Volatile fluxes from Fogo Island. All data in tons/day.

	Summit Fumarolic Field*		Diffuse Degassing <sup>o</sup>		Eruptive degassing (2014 eruption) <sup>£</sup>	Eruptive degassing (time integrated) <sup>§</sup>
	Mean	1 SD	Mean	1 SD	Mean	Mean
SO <sub>2</sub> flux	1.4	0.4	-	-	10118	82
H <sub>2</sub> O flux	780	320	330	-	24245	196
CO <sub>2</sub> flux	1060	340	147-219 (828 <sup>@</sup> )	35-36	10668	86
H <sub>2</sub> S flux	6.2	2.4	0.025	0.007	57	0.5
H <sub>2</sub> flux	0.05	0.022	0.033	0.0105	0.2	0.002

\*This work; <sup>o</sup>inner crater floor; Dionis et al., 2014; <sup>@</sup>whole island; DIONIS *et alii*, 2015; <sup>£</sup>Measured on November 30, 2014; HERNÁNDEZ *et alii*, 2015; <sup>§</sup>This study, recalculated from data in HERNÁNDEZ *et alii*, 2015.

the Differential Optical Absorption Spectroscopy – DOAS - technique) and a Multi-GAS-derived plume composition. Our fumarolic SO<sub>2</sub> output, for example, is a factor ~7000 lower than the large (~10 ktons) daily eruptive release (HERNÁNDEZ *et alii*, 2015). Let emphasize, however, that

while summit fumarolic emissions at Fogo have persisted as a stable degassing feature over the past few centuries (RIBEIRO, 1960), eruptive degassing has been restricted to the relatively infrequent eruptions. There are only 10 reported eruptions since 1785 (RIBEIRO, 1960), of which only 3 since

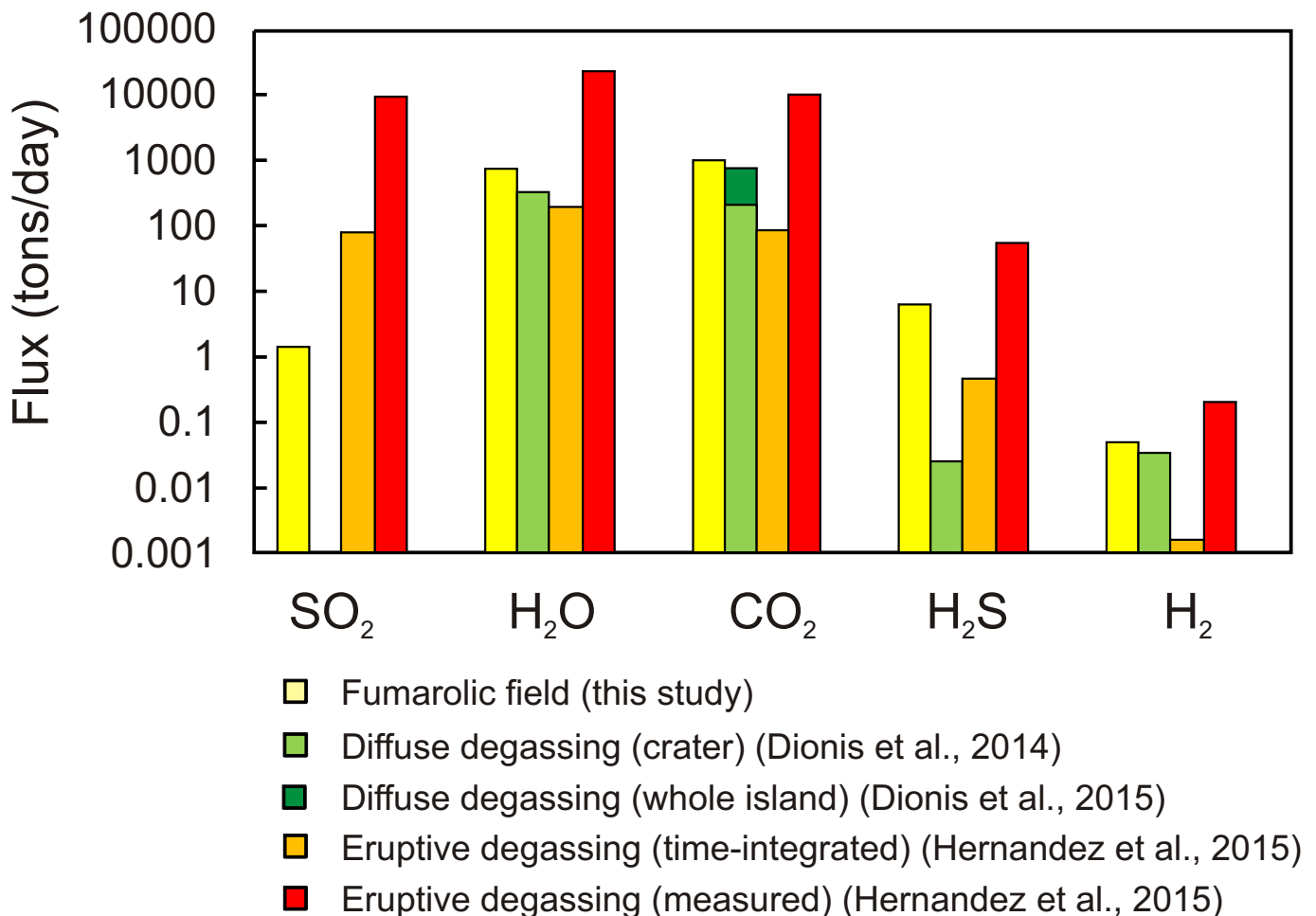


Fig. 8 - Volatile outputs from different types of gas emissions on Fogo Island: (i) the summit fumarolic field, this study; (ii) diffuse soil degassing from the crater area and the whole island (DIONIS *et alii*, 2014, 2015); and (iii) eruptive degassing (HERNÁNDEZ *et alii*, 2015 and recalculated; see text for explanation).

1951 (HILDNER *et alii*, 2011, 2012; CARRACEDO *et alii*, 2015; MATA *et alii*, 2017). Between June 12, 1951 (the onset of the first, well recorded XX century eruption; HILDNER *et alii*, 2012) and February 8, 2015 (the end of the last eruption), Fogo has been in eruption for only 200 days (e.g., 0.008 % of the 24710 elapsed days). If we take the November 30, 2015 gas output (HERNÁNDEZ *et alii*, 2015) as typical for Fogo eruptive daily degassing rate, we can roughly compute a cumulative eruptive release for 1951-2015 (200 days of eruption) of ~4 Mtons of H<sub>2</sub>O, ~2 Mtons of CO<sub>2</sub> and SO<sub>2</sub>, 11 ktons of H<sub>2</sub>S and 0.04 ktons of H<sub>2</sub>. These masses, when scaled to (integrated over) the 24710 days elapsed from June 12, 1951 to February 8, 2015, correspond to daily eruptive outputs of only 196, 86, 82, 0.5 and 0.002 tons/day for H<sub>2</sub>O, CO<sub>2</sub>, SO<sub>2</sub>, H<sub>2</sub>S and H<sub>2</sub>, respectively (Fig. 8). Our back-of-the-envelope calculations demonstrate that, when examined on longer-term perspective, eruptive emissions at Fogo are significant for only SO<sub>2</sub>, while they do make a relatively small contribution to the emission budget of other volatiles (Fig. 8).

We therefore conclude that summit crater fumarolic emissions at Pico do Fogo are the dominant source of volcanic CO<sub>2</sub> (and most other volatiles) over multi-decadal scale.

#### IMPLICATIONS FOR THE GLOBAL CO<sub>2</sub> OUTPUT INVENTORY

On a broader perspective, our results for Pico do Fogo in Cape Verde archipelago add a new piece of information to the global catalogue of volcanic CO<sub>2</sub> emissions. Recent work (FISCHER *et alii*, 2019; WERNER *et alii*, 2019) has attempted at refining the global volcanic CO<sub>2</sub> emission inventory, by reviewing, cataloguing and synthesizing the volcanic CO<sub>2</sub> output information available in the international literature. It was found that, by late 2019, CO<sub>2</sub> flux measurements have become available for 102 of the ~500 degassing subaerial volcanoes worldwide (FISCHER *et alii*, 2019; WERNER *et alii*, 2019; FISCHER & AIUPPA, 2020 submitted). Different strategies have been used to extrapolate the cumulative CO<sub>2</sub> output “measured” for the 102 volcanoes (~44 Tg/yr) to CO<sub>2</sub> emissions from the several hundred “unmeasured” subaerial degassing volcanoes. These have included the use of independent rock-chemistry information (AIUPPA *et alii*, 2019) and/or the identification of statistical properties (mean CO<sub>2</sub> output and confidence intervals) for different categories of volcanoes. On the latter basis, it was proposed that the present-day global volcanic CO<sub>2</sub> budget is dominated by the category of Strong Volcanic Gas Emitters (S<sub>vge</sub>) – which includes the ~100 top degassing volcanoes whose SO<sub>2</sub> emissions are

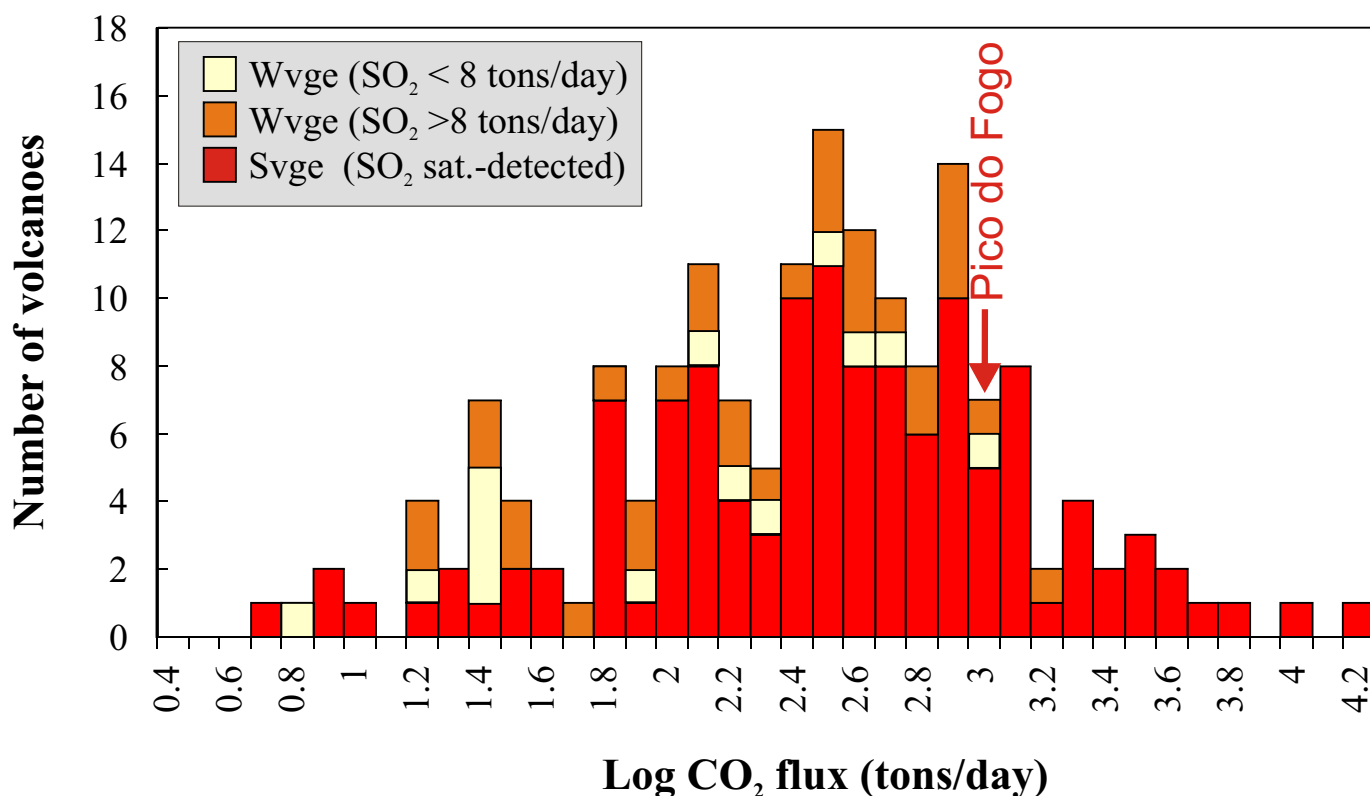


Fig. 9 - Histogram showing the logarithmic distribution of the population of measured/predicted CO<sub>2</sub> fluxes (in tons/day) from subaerial volcanoes. Data are from Fischer *et alii*, (2019) except for Pico do Fogo (this study). Following FISCHER *et alii*, (2019) and FISCHER & AIUPPA (2019, submitted), volcanoes are distinguished in two sub-categories: 1) Strong Volcanic Gas Emitters (S<sub>vge</sub>, in red), including the 125 top degassing volcanoes whose SO<sub>2</sub> emissions have systematically been detected from space-borne and/or ground-based spectrometers (CARN *et alii*, 2017; FISCHER *et alii*, 2019); and 2) Weak Volcanic Gas Emitters (W<sub>vge</sub>), including volcanoes with no visible plumes and weak SO<sub>2</sub> emissions. Like in FISCHER *et alii*, (2019) and FISCHER & AIUPPA, (2020, submitted), W<sub>vge</sub> are further divided into hydrothermal volcanoes, with minor to absent (< 8 tons/day) SO<sub>2</sub> emissions (yellow), and magmatic-hydrothermal volcanoes with somewhat higher (> 8 tons/day, but still undetectable from space) SO<sub>2</sub> emissions (orange). Fogo, although falling in the subcategory of W<sub>vge</sub> (SO<sub>2</sub> < 8 tons/day) emits CO<sub>2</sub> at the upper W<sub>vge</sub> range, and at levels comparable to (or higher than) many S<sub>vge</sub>.

systematically detected from space-borne and/or ground-based spectrometers (CARN *et alii*, 2017; FISCHER *et alii*, 2019).  $S_{\text{vge}}$  have an inferred total (extrapolated)  $\text{CO}_2$  output of ~ 36–39 Tg/yr (AIUPPA *et alii*, 2019; FISCHER *et alii*, 2019). It was additionally found that a group of Weak Volcanic Gas Emitters ( $W_{\text{vge}}$ ), although degassing in a more subtle manner (this category includes volcanoes with no visible plumes and/or minor to absent  $\text{SO}_2$  emissions), may still contribute between 15 (FISCHER *et alii*, 2019) and 35 (WERNER *et alii*, 2019) Tg  $\text{CO}_2$ /yr, simply because they are numerous (~400) globally. Unfortunately, however, these results are subject to very large uncertainties because measuring the  $\text{CO}_2$  output from quiescent/hydrothermal volcanoes is especially challenging from a technical viewpoint (indirect  $\text{SO}_2$  flux-based estimates are hampered by low to absent  $\text{SO}_2$ ; WERNER *et alii*, 2019), making the  $\text{CO}_2$  flux catalogue particularly incomplete for  $W_{\text{vge}}$ .

Pico do Fogo falls within the  $W_{\text{vge}}$  category, as no plume is visually observable (Fig. 2) and no  $\text{SO}_2$  is detectable by satellite except during the infrequent eruptions (GLOBAL VOLCANISM PROGRAM, 2017). Our results show, however, that  $\text{SO}_2$  is present in tiny but measurable quantities in the fumaroles (Table 1), making both the  $\text{SO}_2$  flux and, indirectly, the  $\text{CO}_2$  flux (Table 3) measurable from a very proximal location on ground (Fig. 2; note that a test made with UV-Camera from the base of the volcano were unable to detect any  $\text{SO}_2$  release).

When put in the context of global volcanic  $\text{CO}_2$  fluxes (Fig. 9; data from FISCHER *et alii*, 2019), the fumarolic  $\text{CO}_2$  flux from Pico do Fogo (ca. 1000 tons/day) confirms that  $W_{\text{vge}}$  volcanoes can emit  $\text{CO}_2$  in quantities that, in some cases, can rival the emissions of  $S_{\text{vge}}$  volcanoes. High  $\text{CO}_2$  emission from such  $W_{\text{vge}}$  systems, despite negligible (hydrothermal-dominant) to weak (magmatic-hydrothermal)  $\text{SO}_2$  emission (FISCHER *et alii*, 2019), result from their exceptionally high  $\text{CO}_2/S_{\text{t}}$  signature (AIUPPA *et alii*, 2017). Pico do Fogo fumaroles are not an exception, but owing to their high  $\text{CO}_2/S_{\text{t}}$  compositions they can sustain a  $\text{CO}_2$  output of order 1000 tons/day, at the upper range of the global  $W_{\text{vge}}$  and  $S_{\text{vge}}$  populations (Fig. 9). Therefore, our present results further demonstrate that refining the global inventory for volcanic  $\text{CO}_2$  output will require enhanced quantification of the weaker, poorly visible emissions sustained by quiescent hydrothermal volcanoes, the majority of which still lack  $\text{CO}_2$  flux quantification.

## CONCLUSIONS

We have shown here that fumarolic activity on-top of Fogo Volcano, in the Atlantic Cape Verde Archipelago, is currently a poorly visible but substantial source of volcanic volatiles to the atmosphere. The fumarolic  $\text{CO}_2$  output (~1060 tons/day), in particular, is found to exceed by far the time-integrated eruptive  $\text{CO}_2$  flux (~86 tons/day) from the volcano, as well as the estimated total  $\text{CO}_2$  budget from soil degassing across Fogo Island (147–828 tons/day). On a broader scale, our results confirm that quiescent volcanoes characterized by hydrothermal activity during quiescent stages can produce  $\text{CO}_2$  emissions that rival those of more manifestly degassing (Strong Volcanic Gas Emitters,  $S_{\text{vge}}$ ) owing to their  $\text{CO}_2$ -enriched fumarole compositions ( $\text{CO}_2/S_{\text{t}}$  ratios of 93–163 at Pico do Fogo in 2019). At Pico do Fogo, these  $\text{CO}_2$ -enriched compositions likely result

from the interactions (scrubbing of magmatic sulphur, and water condensation) of a deep magmatic gas supply (perhaps sourced from a 16–28 km deep magma reservoir in the uppermost mantle; HILDNER *et alii*, 2011, 2012; MATA *et alii*, 2017) with a shallow hydrothermal system.

## ACKNOWLEDGEMENTS

This research was funded by the Portuguese Fundação para a Ciência e a Tecnologia (MARES project - PTDC/GEO-FIQ/1088/2014), the DECADE project of the Deep Carbon Observatory, and the Italian Ministero Istruzione Università e Ricerca (Grant n. 2017LMNLAW). We thank Francesco Salerno and Manfredi Longo from INGV-Palermo for providing support with gas chromatographic analysis. The manuscript benefited from constructive reviews from Taryn Lopez, Yuri Taran and from the Associate Editor Orlando Vaselli.

## REFERENCES

- AIUPPA A. (2015) - *Volcanic-gas monitoring* In: SCHMIDT A., KIRTSSEN F. & ELKINS-TANTON L. (Eds.) - *Volcanism and global environmental change*, pp. 81–96. Cambridge University Press. <https://doi.org/10.1017/CBO9781107415683.009>
- AIUPPA A., FEDERICO C., GIUDICE G. & GURRIERI S. (2005a) - *Chemical mapping of a fumarolic field: La Fossa Crater, Vulcano Island (Aeolian Islands, Italy)*. *Geophys. Res. Lett.*, **32**, 4.
- AIUPPA A., INGUAGGIATO S., MCGONIGLE A.J.S., O'DWYER M., OPPENHEIMER C., PADGETT M.J., ROUWET D. & VALENZA M. (2005b) -  *$H_2S$  fluxes from Mt. Etna, Stromboli, and Vulcano (Italy) and implications for the sulfur budget at volcanoes*. *Geochim. Cosmochim. Acta*, **69**(7), 1861–1871.
- AIUPPA A., SHINOHARA H., TAMBURELLO G., GIUDICE G., LIUZZO M. & MORETTI R. (2011) - *Hydrogen in the gas plume of an open-vent volcano, Mount Etna, Italy*. *J. Geophys. Res. B: Solid Earth*, **116**(10), B10204.
- AIUPPA A., FIORANI L., SANTORO S., PARRACINO S., NUvoli M., CHIODINI G., MINOPOLI C. & TAMBURELLO G. (2015) - *New ground-based lidar enables volcanic  $\text{CO}_2$  flux measurements*. *Sci. Reports*, **5**, 13614.
- AIUPPA A., LO COCO E., LIUZZO M., GIUDICE G., GIUFFRIDA G. & MORETTI R. (2016) - *Terminal Strombolian activity at Etna's central craters during summer 2012: The most  $\text{CO}_2$ -rich volcanic gas ever recorded at Mount Etna*. *Geochemical Journal*, **50**(2), 123–138.
- AIUPPA A., FISCHER T.P., PLANK T., ROBIDOUX P. & DI NAPOLI R. (2017) - *Along-arc, interarc and arc-to-arc variations in volcanic gas  $\text{CO}_2/S_{\text{t}}$  ratios reveal dual source of carbon in arc volcanism*. *Earth Science Reviews*, **168**, 24–47.
- AIUPPA A., FISCHER T.P., PLANK T. & BANI P. (2019) -  *$\text{CO}_2$  flux emissions from the Earth's most actively degassing volcanoes, 2005–2015*. *Sci. Reports*, **9**, 5442. <https://doi.org/10.1038/s41598-019-41901-y>
- ALLARD P., AIUPPA A., BEAUDICEL, GAUDIN D., DI NAPOLI R., CRISPI O., CALABRESE S., PARELLO F., HAMMOUYA G. & TAMBURELLO G. (2014) - *Steam and gas emission rate from La Soufriere volcano, Guadeloupe (Lesser Antilles): implications for the magmatic supply during degassing unrest*. *Chemical Geology*, **384**, 76–93
- ASIMOW P.D., DIXON J.E. & LANGMUIR C.H. (2004) - *A hydrous melting and fractionation model for mid-ocean ridge basalts: application to the Mid-Atlantic Ridge near the Azores*. *Geochemistry, Geophysics, Geosystems*, **5**. <https://doi.org/10.1029/2003GC000568>
- BONATTI E. (1990) - *Not so hot 'hot spots' in the oceanic mantle*. *Science*, **250**, 107–111.
- BRUNE S., WILLIAMS S.E. & MÜLLER R.D. (2017) - *Potential links between continental rifting,  $\text{CO}_2$  degassing and climate change through time*. *Nat. Geosci.*, **10**, 941–946. <https://doi.org/10.1038/s41561-017-0003-6>
- CALIRO S., VIVEIROS F., CHIODINI G. & FERREIRA T. (2015) - *Gas geochemistry of hydrothermal fluids of the S. Miguel and Terceira Islands, Azores*. *Geochimica et Cosmochimica Acta*, **168**, 43–57. <https://doi.org/10.1016/j.gca.2015.07.009>
- CAPPELLO A., GANCI G., CALVARI S., PÉREZ N.M., HERNÁNDEZ P.A., SILVA S.V., CABRAL J. & DEL NEGRO C. (2016) - *Lava flow hazard modeling during the 2014–2015 Fogo eruption, Cape Verde*. *Journal of Geophysical Research: Solid Earth*, **121**(4), 2290–2303.

- CARN S.A., FIOLETOV V.E., MCLINDEN C.A., LI C. & KROTKOV N.A. (2017) - *A decade of global volcanic SO<sub>2</sub> emissions measured from space*. Sci. Reports, **7**, 44095. <https://doi.org/10.1038/srep44095>
- CARRACEDO J.-C., PEREZ-TORRADO F.J., RODRIGUEZ-GONZALEZ A., PARIS R., TROLL V.R. & BARKER A.K. (2015) - *Volcanic and structural evolution of Pico do Fogo, Cape Verde*. Geology Today, **31**(4), 146-152.
- CHIODINI G. & MARINI L. (1998) - *Hydrothermal gas equilibria: The H<sub>2</sub>O-H<sub>2</sub>-CO<sub>2</sub>-CO-CH<sub>4</sub> system*. Geochim. Cosmochim. Acta, **62**(15), 2673-2687. [https://doi.org/10.1016/S0016-7037\(98\)00181-1](https://doi.org/10.1016/S0016-7037(98)00181-1)
- CHRISTENSEN B., HOLM P., JAMBON A. & WILSON J. (2001) - *Helium, argon and lead isotopic composition of volcanics from Santo Antão and Fogo, Cape Verde Islands*. Chemical Geology, **178**, 127-142.
- COURTNEY R.C. & WHITE R.S. (1986) - *Anomalous heat-flow and geoid across the Cape Verde rise — evidence for dynamic support from a thermal plume in the mantle*. Geophysical Journal International, **87**(3), 815-867.
- CROUGH S.T. (1978) - *Thermal origin of mid-plate hot-spot swells*. Geophys. J. R. Astron. Soc., **55**, 451-469.
- CROUGH S.T. (1982) - *Geoid anomalies over the Cape Verde Rise*. Mar. Geophys. Res., **5**, 263-271. <https://doi.org/10.1007/BF00305564>
- DASGUPTA R. (2013) - *Ingassing, storage, and outgassing of terrestrial carbon through geologic time*. Rev. Mineral. Geochem., **75**, 183-229. <https://doi.org/10.2138/rmg.2013.75.7>
- DASGUPTA R. & HIRSCHMANN M.M. (2010) - *The deep carbon cycle and melting in Earth's interior*. Earth Planet. Sci. Lett., **298**, 1-13. <https://doi.org/10.1016/j.epsl.2010.06.039>
- DAVIES G.F., NORRY M.J., GERLACH D.C. & CLIFF R.A. (1989) - *A combined chemical and Pb-Sr-Nd isotope study of the Azores and Cape Verde hotspots: The geodynamic implications, in Magmatism in the Ocean Basins*. Geol. Soc. Spec. Publ., **42**, 231-255.
- DAY S.J., HELENO DA SILVA S.I.N. & FONSECA J.F.B.D. (1999) - *A past giant lateral collapse and present-day flank instability of Fogo, Cape Verde Islands*. Journal of Volcanology and Geothermal Research, **94**(1-4), 191-218.
- DAY S.J., CARRACEDO J., GUILLOU H., PAIS PAIS F., RODRIGUEZ BADIOLA E., FONSECA J. & HELENO DA SILVA S. (2000) - *Comparison and cross-checking of historical, archaeological and geological evidence for the location and type of historical and sub-historical eruptions of multiple-vent oceanic island volcanoes*. In: MCGUIRE W., GRIFFITHS D., HANCOCK P., STEWART I. (Eds.), *The Archaeology of Geological Catastrophes*: Geological Society, London, Special Publications, London, pp. 281-306.
- DELLE DONNE D., AIUPPA A., BITETTO M., D'ALEO R., COLTELLI M., COPPOLA D., PECORA E., RIPEPE M. & TAMBURELLO G. (2019) - *Changes in SO<sub>2</sub> flux regime at Mt. Etna captured by automatically processed ultraviolet camera data*. Remote Sensing, **11**(10), art. no. 1201.
- DIONIS S.M., MELIÁN G., RODRÍGUEZ F., HERNÁNDEZ P.A., PADRÓN E., PÉREZ N.M., BARRANCOS J., PADILLA G., SUMINO H., FERNANDES P., BANDOMO Z., SILVA S., PEREIRA J.M. & SEMEDO H. (2014) - *Diffuse volcanic gas emission and thermal energy release from the summit crater of Pico do Fogo, Cape Verde*. Bulletin of Volcanology, **77**(2), 13 p.
- DIONIS S.M., PÉREZ N.M., HERNÁNDEZ P.A., MELIÁN G., RODRÍGUEZ F., PADRÓN E., SUMINO H., BARRANCOS J., PADILLA G.D., FERNANDES P., BANDOMO Z., SILVA S., PEREIRA J.M., SEMEDO, H. & CABRAL J. (2015) - *Diffuse CO<sub>2</sub> degassing and volcanic activity at Cape Verde Islands, West Africa*. Earth, Planets and Space, **67**(1), art. no. 48.
- DOUCELANCE R., ESCRIG S., MOREIRA M., GARIPEY C. & KURZ M.D. (2003) - *Pb-Sr-He isotope and trace element geochemistry of the Cape Verde Archipelago*. Geochim. Cosmochim. Acta, **67**, 3717-3733.
- FERREIRA T. & OSKARSSON N. (1999) - *Chemistry and isotopic composition of fumarole discharges of Furnas caldera*. J. Volcanol. Geotherm. Res., **92**, 169-179.
- FERREIRA T., GASPAR J.L., VIVEIROS F., MARCOS M., FARIA C. & SOUSA F. (2005) - *Monitoring of fumarole discharge and CO<sub>2</sub> soil degassing in the Azores: contribution to volcanic surveillance and public health risk assessment*. Ann. Geophys., **48**, 787-796.
- FISCHER T.P. (2013) - *DEep Carbon DEgassing: The Deep Carbon Observatory DECADE Initiative*. Mineralogical Magazine, **77**(5), 1089.
- FISCHER T.P. & AIUPPA A. (2020) - *Global CO<sub>2</sub> emissions from subaerial volcanism: recent progresses and future challenges*. Geochim. Geophys., **21**(3), e2019GC008690.
- FISCHER T.P. & CHIODINI G. (2015) - *Volcanic, Magmatic and Hydrothermal Gases*. In: The Encyclopedia of Volcanoes, 2nd Edition, Edited by H. Sigurdsson, B. Houghton, S. McNutt, H. Rymer, J. Stix Elsevier. <https://doi.org/10.1016/B978-0-12-385938-9.00045-6>
- FISCHER T.P., ET ALII (2019) - *The emissions of CO<sub>2</sub> and other volatiles from the world's subaerial volcanoes*. Sci. Rep., **9**, 18716. <https://doi.org/10.1038/s41598-019-54682-1>
- GERLACH D.C., CLIFF C.A., DAVIES G.R., NORRY M.J. & HODGSON N. (1988) - *Magma sources of the Cape Verdes archipelago: Isotopic and trace element constraints*. Geochim. Cosmochim. Acta, **52**, 2979-2992. [https://doi.org/10.1016/0016-7037\(88\)90162-7](https://doi.org/10.1016/0016-7037(88)90162-7)
- GERLACH T.M. (1991) - *Present-day carbon dioxide emissions from volcanoes*. Earth in Space, **4**, 5.
- GLOBAL VOLCANISM PROGRAM, 2017. REPORT ON FOGO (Cape Verde). In: Crafford A.E. & Venzke E. (eds.), Bulletin of the Global Volcanism Network, **42**, 9. Smithsonian Institution. <https://doi.org/10.5479/si.GVP.BGVN201709-384010>
- GIGGENBACH W.F. (1987) - *Redox processes governing the chemistry of fumarolic gas discharges from White Island, New Zealand*. Appl. Geochem., **2**, 143-161. [https://doi.org/10.1016/0883-2927\(87\)90030-8](https://doi.org/10.1016/0883-2927(87)90030-8)
- HERNÁNDEZ P.A. (2015) - *Chemical composition of volcanic gases emitted during the 2014-15 Fogo eruption, Cape Verde*. Geophysical Research Abstracts, **17**, EGU2015-9577, 2015, EGU General Assembly 2015.
- HILDNER E., KLÜGEL A. & HAUFF F. (2011) - *Magma storage and ascent during the 1995 eruption of Fogo, Cape Verde Archipelago*. Contributions to Mineralogy and Petrology, **162**(4), 751. <https://doi.org/10.1007/s00410-011-0623-6>
- HILDNER H., KLÜGEL A. & HANSTEEN T. (2012) - *Barometry of lavas from 1951 eruption of Fogo, Cape Verde Islands: implications for historic and prehistoric magma plumbing system*. Journal of Volcanology and Geothermal Research, **217-218**, 73-90.
- HOERNLE K., TILTON G., LE BAS M.J., DUGGEN S. & GARBE-SCHÖNBERG D. (2002) - *Geochemistry of oceanic carbonatites compared with continental carbonatites: mantle recycling of oceanic crustal carbonate*. Contributions to Mineralogy and Petrology, **142**(5), 520-542.
- HOLM P.M., WILSON J.R., CHRISTENSEN B.P., HANSEN L., HANSEN S.L., HEIN K.M., MORTENSEN A.K., PEDERSEN R., PLESNER S. & RUNGE M.K. (2006) - *Sampling the Cape Verde mantle plume: evolution of the melt compositions on Santo Antão, Cape Verde Islands*. Journal of Petrology, **47**, 145-189.
- HOLM P.M., GRANDVUINET T., FRIIS J., WILSON J.R., BARKER A.K. & PLESNER S. (2008) - *An <sup>40</sup>Ar-<sup>39</sup>Ar study of the Cape Verde hot spot: temporal evolution in a semistationary plate environment*. Journal of Geophysical Research, **113**(B8), B08201.
- KANTZAS E.P., MCGONIGLE A.J.S., TAMBURELLO G., AIUPPA A. & BRYANT R.G. (2010) - *Protocols for UV camera volcanic SO<sub>2</sub> measurements*. J. Volcanol. Geotherm. Res., **194**, 55-60.
- KERN C., KICK F., LÜBCKE P., VOGEL L., WÖHRBACH M. & PLATT U. (2010) - *Theoretical description of functionality, applications, and limitations of SO<sub>2</sub> cameras for the remote sensing of volcanic plumes*. Atmos. Meas. Tech., **3**, 733-749. <https://doi.org/10.5194/amt-3-733-2010>
- KOGARKO L.N., RYABUKHIN V.A. & VOLYNETS M.P. (1992) - *Cape Verde Island carbonatite geochemistry*. Geochem. Int., **29**, 62-74.
- ILYINSKAYA E., AIUPPA A., BERGSSON B., DI NAPOLI R., FRIDRIKSSON T., OLADOTTIR A.A., ÓSKARSSON F., GRASSA F., PFEFFER M., LECHNER K. & YEO R. (2015) - *Degassing regime of Hekla volcano 2012-2013*. Geochim. Cosmochim. Acta, **159**, 80-99.
- ILYINSKAYA E., MOBBS S., BURTON R., BURTON M., PARDINI F., PFEFFER M.A., PURVIS R., LEE J., BAUGUITTE S., BROOKS B., COLFESCU I., PETERSEN G.N., WELLPOTT A. & BERGSSON B. (2018) - *Globally significant CO<sub>2</sub> emissions from Katla, a Subglacial Volcano in Iceland*. Geophys. Res. Lett., **45**, 332-310. <https://doi.org/10.1029/2018GL079096>
- LIU X. & ZHAO D. (2014) - *Seismic evidence for a mantle plume beneath the Cape Verde hotspot*. International Geology Review, **56**, 1213-1225.
- LOPEZ T., TASSI F., AIUPPA A., GALLE B., RIZZO A.L., FIEBIG J., CAPECCHIACCI F., GIUDICE G., CALIRO S. & TAMBURELLO G. (2017) - *Geochemical constraints on volatile sources and subsurface conditions at Mount Martin, Mount Mageik, and Trident Volcanoes, Katmai*. J. Volcanol. Geotherm. Res., **347**, 64-81. <https://doi.org/10.1016/j.jvolgeores.2017.09.001>

- MARQUES F.O., CATALÃO J.C., DEMETS C., COSTA A.C.G. & HILDENBRAND A. (2013) - *GPS and tectonic evidence for a diffuse plate boundary at the Azores Triple Junction*. *Earth and Planetary Science Letters*, **381**, 177-187.
- MARQUES F.O., HILDENBRAND A., VICTÓRIA S.S., CUNHA D. & DIAS, P. (2020) - *Caldera or flank collapse in the Fogo volcano? What age? Consequences for risk assessment in volcanic islands*. *Journal of Volcanology and Geothermal Research*, **338**. <https://doi.org/10.1016/j.jvolgeores.2019.106686>
- MATA J., MOREIRA M., DOUCELANCE R., ADER M. & SILVA, L.C. (2010) - *Noble gas and carbon isotopic signatures of Cape Verde oceanic carbonatites: implications for carbon provenance*. *Earth and Planetary Science Letters*, **291**, 70–83.
- MATA J., MARTINS S., MATTIELLI N., MADEIRA J., FARIA B., RAMALHO R.S., SILVA P., MOREIRA M., CALDEIRA R., RODRIGUES J. & MARTINS L. (2017) - *The 2014–15 eruption and the short-term geochemical evolution of the Fogo volcano (Cape Verde): Evidence for small-scale mantle heterogeneity*. *Lithos*, **288-289**, 91–107.
- MELIÁN G., TASSI F., PÉREZ N., HERNÁNDEZ P., SORTINO F., VASELLI O., PADRÓN E., NOLASCO D., BARRANCOS J., PADILLA G., RODRÍGUEZ F., DIONIS S., CALVO D., NOTSU K. & SUMINO H. (2012) - *A magmatic source for fumaroles and diffuse degassing from the summit crater of Teide Volcano (Tenerife, Canary Islands): A geochemical evidence for the 2004-2005 seismic-volcanic crisis*. *Bulletin of Volcanology*, **74**(6), 1465-1483.
- MELIÁN G.V., DIONIS S., ASENSIO-RAMOS M., PADILLA G., FERNANDES P., PÉREZ N.M., SUMINO H., PADRÓN E., HERNÁNDEZ P.A., SILVA S., PEREIRA J.M., SEMEDO H. & CABRAL J. (2015) - *Insights from fumarole gas geochemistry on the recent volcanic unrest of Pico do Fogo, Cape Verde*. *Geophysical Research Abstracts*, **17**, EGU2015-12754, 2015, EGU General Assembly 2015.
- MÉTRICH N., ZANON V., CRÉON L., HILDENBRAND A., MOREIRA M. & MARQUES F.O. (2014) - *Is the "Azores hotspot" a wet spot? Insights from geochemistry of fluid and melt inclusions in olivines of Pico basalts*. *J. Petrol.*, **55**, 377-393
- MILLET M.A., DOUCELANCE R., SCHIANO P., DAVID K. & BOSQ C. (2008) - *Mantle plume heterogeneity versus shallow-level interactions: a case study, the São Nicolau Island, Cape Verde archipelago*. *Journal of Volcanology and Geothermal Research*, **176**(2), 265-276.
- MONTELLI R., NOLET G., DAHLEN F.A. & MASTERS G. (2006) - *A catalogue of deep mantle plumes: new results from finite-frequency tomography*. *Geochemistry, Geophysics, Geosystems*, **7**, <http://dx.doi.org/10.1029/2006GC001248>
- MOURÃO C., MOREIRA M., MATA J., RAQUIN A. & MADEIRA J. (2012) - *Primary and secondary processes constraining the noble gas isotopic signatures of carbonatites and silicate rocks from Brava Island: evidence for a lower mantle origin of the Cape Verde plume*. *Contributions to Mineralogy and Petrology*, **163**, 995–1009.
- PEDONE M. ET ALII (2014) - *Volcanic CO<sub>2</sub> flux measurement at Campi Flegrei by tunable diode laser absorption spectroscopy*. *Bulletin of Volcanology*, **76**, 13.
- QUEISSER M., GRANIERI D. & BURTON M. (2016) - *A new frontier in CO<sub>2</sub> flux measurements using a highly portable DIAL laser system*. *Scientific Reports*, **6**, 33834.
- RIBEIRO O. (1960) - *A Ilha do Fogo e as suas erupções (The island of Fogo and its eruptions)*. 2<sup>nd</sup> edn. *Memórias, serie geographica I*. Junta de Investigações do Ultramar. Ministerio do Ultramar, Lisbon.
- RICHTER N., FAVALLI M., DE ZEEUW-VAN DALFSEN E., FORNACIAI A., DA SILVA FERNANDES R.M., PÉREZ N.M., LEVY J., VICTÓRIA S.S. & WALTER T.R. (2016) - *Lava flow hazard at Fogo Volcano, Cabo Verde, before and after the 2014-2015 eruption*. *Natural Hazards and Earth System Sciences*, **16**(8), pp. 1925-1951.
- SAKI M., THOMAS C., NIPPRESS S.E.J. & LESSING S. (2015) - *Topography of upper mantle seismic discontinuities beneath the North Atlantic: the Azores, Canary and Cape Verde plumes*. *Earth and Planetary Science Letters*, **409**, 193–202.
- TAMBURELLO G. (2015) - *Ratiocalc: Software for processing data from multicomponent volcanic gas analyzers*. *Comput. Geosci.*, **82**, 63–67.
- TAMBURELLO G., KANTZAS E.P., MCGONIGLE A.J.S. & AIUPPA A. (2011) - *Vulcamera, a program for measuring volcanic SO<sub>2</sub> using UV cameras*. *Ann. Geophys.* **54**, 2.
- TAMBURELLO G., AIUPPA A., KANTZAS E.P., MCGONIGLE A.J.S. & RIPEPE M. (2012) - *Passive vs. active degassing modes at an open-vent volcano (Stromboli, Italy)*. *Earth Planet. Sci. Lett.*, **359-360**, 106–116.
- TAMBURELLO G., MOUNE S., ALLARD P., VENUGOPAL S., ROBERT V., ROSAS-CARNAJAL M., UCCIANI G., DEROUSSI S., KITOU T., DIDIER T., KOMOROWSKI J-C., BEAUDICEL F., DE CHABALIER J-B., LEMARCHAND A., MORETTI R. & DESSERT C. (2019) - *Spatio-temporal relationships between fumarolic activity, hydrothermal fluid circulation and geophysical signals at an arc volcano in degassing unrest: La Soufrière of Guadeloupe (French West Indies)*. *Geosciences*, **9**, 480-507. <https://doi.org/10.3390/geosciences9110480>
- TARAN Y. & KALACHEVA E. (2019) - *Role of hydrothermal flux in the volatile budget of a subduction zone: Kuril arc, northwest Pacific*. *Geology*, **47**(1), 87-90. <https://doi.org/10.1130/G45559.1>
- TARAN Y.A. (2009) - *Geochemistry of volcanic and hydrothermal fluids and volatile budget of the Kamchatka-Kuril subduction zone*. *Geochimica et Cosmochimica Acta*, **73**(4), 1067-1094, <https://doi.org/10.1016/j.gca.2008.11.020>
- VAN DER MEER D.G., ZEEBE R.E., VAN HINSBERGEN D.J.J., SLUIJS A., SPAKMAN W. & TORSVIK T.H. (2014) - *Plate tectonic controls on atmospheric CO<sub>2</sub> levels since the Triassic*. *Proc. Natl. Acad. Sci. U.S.A.*, **111**, 4380–4385. <https://doi.org/10.1073/pnas.1315657111>
- WERNER C., EVANS W.C., POLAND M., TUCKER D.S. & DOUKAS M.P. (2009) - *Long-term changes in quiescent degassing at Mount Baker Volcano, Washington, USA; evidence for a stalled intrusion in 1975 and connection to a deep magma source*. *Journal of Volcanology and Geothermal Research*, **186**, 379–386.
- WERNER C., FISCHER T.P., AIUPPA A., EDMONDS M., CARDELLINI C., CARN S., CHIODINI G., COTTRELL E., BURTON M., SHINOHARA H. & ALLARD P. (2019) - *Carbon Dioxide Emissions from Subaerial Volcanic Regions: Two Decades in Review*. In: ORCUTT B.N., DANIEL I. & DASGUPTA R. (Eds.) *Deep Carbon, Past to Present*. Cambridge University Press [www.cambridge.org/9781108677950](https://doi.org/10.1017/9781108677950), <https://doi.org/10.1017/9781108677950>
- WONG K., MASON E., BRUNE S, EAST M., EDMONDS M. & ZAHROVIC S. (2019) - *Deep Carbon Cycling Over the Past 200 Million Years: A Review of Fluxes in Different Tectonic Settings*. *Front. Earth Sci.*, **7**, 263. <https://doi.org/10.3389/feart.2019.00263>